PHYSICAL REVIEW D **92,** 015014 (2015)

$SU(5)$-inspired double beta decay

Renato M. Fonseca[*] and Martin Hirsch[†]

AHEP Group, Instituto de Física Corpuscular–C.S.I.C./Universitat de València
Edificio Institutos de Investigación, E–46071 València, Spain

(Received 1 June 2015; published 14 July 2015)

The short-range part of the neutrinoless double beta amplitude is generated via the exchange of exotic particles, such as charged scalars, leptoquarks and/or diquarks. In order to give a sizable contribution to the total decay rate, the masses of these exotics should be of the order of (at most) a few TeV. Here, we argue that these exotics could be the "light" (i.e., weak-scale) remnants of some $B-L$ violating variants of $SU(5)$. We show that unification of the standard model gauge couplings, consistent with proton decay limits, can be achieved in such a setup without the need to introduce supersymmetry. Since these nonminimal $SU(5)$-inspired models violate $B-L$, they generate Majorana neutrino masses and therefore make it possible to explain neutrino oscillation data. The light colored particles of these models can potentially be observed at the LHC, and it might be possible to probe the origin of the neutrino masses with $\Delta L=2$ violating signals. As particular realizations of this idea, we present two models, one for each of the two possible tree-level topologies of neutrinoless double beta decay.

DOI: 10.1103/PhysRevD.92.015014 PACS numbers: 23.40.-s, 12.10.Dm, 14.60.Pq, 95.35.+d

I. INTRODUCTION

Neutrinoless double beta decay ($0\nu\beta\beta$) is usually considered as a probe to constrain (or measure) the Majorana neutrino mass scale. However, a nonzero amplitude for $0\nu\beta\beta$ decay is generated in any extension of the standard model with lepton number violation (for a recent review see, for example [1]) and, in general, the mass mechanism is not necessarily the dominant contribution to the decay rate.

The short-range part of the $0\nu\beta\beta$ decay rate [2] is generated via the exchange of exotic particles, such as leptoquarks and/or diquarks plus possibly some exotic fermions. The "heavy" mediators in these diagrams must have masses of at most a few TeV in order to give a sizable contribution to the $0\nu\beta\beta$ decay rate, and thus they can potentially be produced and studied at the LHC [3,4]. A complete list of all (scalar-) mediated short-range contributions to $0\nu\beta\beta$ decay has been given in [5]. One can understand the results of this work [5] as a *bottom-up* reconstruction of all possible particle physics models with tree-level $0\nu\beta\beta$ decay. In this paper we take the opposite approach and study instead the $0\nu\beta\beta$ decay in a *top-down* approach; in other words, we explore the possibility that some of these exotics could be the "light" remnants of multiplets in some unified theory.

Minimal $SU(5)$ accidentally conserves $B-L$ [6]. Once $SU(5)$ is broken to the standard model group ($G_{\rm SM}$), baryon number violating processes such as proton decay occur, but the combination $B-L$ is still conserved. Thus, neutrinos are as massless in minimal $SU(5)$ as in the standard model (SM) and remain so also after $SU(5)$ breaking. Adding $SU(5)$ singlets a type-I seesaw mechanism [7–10] can be generated. While certainly theoretically attractive to many, this scenario leaves as its only prediction that neutrinoless double beta decay should be observed.[1]

Allowing for larger $SU(5)$ multiplets, however, $B-L$ is no longer conserved in $SU(5)$. Perhaps adding a scalar **15** is the simplest way to obtain a model with $B-L$ violation *in the $SU(5)$ symmetric phase*. Indeed, it is possible to write down the Yukawa interaction $\bar{\mathbf{5}}_F \cdot \mathbf{15} \cdot \bar{\mathbf{5}}_F$ as well as a scalar trilinear term $\mathbf{5} \cdot \mathbf{15}^* \cdot \mathbf{5}$, with the $\bar{\mathbf{5}}_F$ containing the SM d^c and L fermion fields and the **5** containing the SM Higgs doublet H. In terms of $G_{\rm SM}$ representations, we have both the $LLS_{\mathbf{1},\mathbf{3},1}$ and $HHS^*_{\mathbf{1},\mathbf{3},1}$ interactions, where $S_{\mathbf{1},\mathbf{3},1} \subset \mathbf{15}$,[2] therefore a type-II seesaw [11–14] will be generated, yielding the effective operator $LLHH$ [or $\bar{\mathbf{5}}_F \cdot \bar{\mathbf{5}}_F \cdot \mathbf{5} \cdot \mathbf{5}$ in terms of $SU(5)$ fields]. Many other examples of $B-L$ violating $SU(5)$ models can be constructed using larger representations.

Extrapolating the SM gauge couplings to larger energies with only the SM particle content fails to achieve unification. Thus, no consistent model of grand unification can be built without adding new particles and/or interactions at some so-far unexplored energy scale. One of the most cited possibility to achieve gauge coupling unification (GCU) is to extend the SM to the minimal supersymmetric standard model [15]. However, it has been known for a long time that also many nonsupersymmetric scenarios can lead to

[*]renato.fonseca@ific.uv.es
[†]mahirsch@ific.uv.es

[1]Albeit without fixing the $0\nu\beta\beta$ decay half-life, unless further assumptions about the active neutrino mass spectrum are made.

[2]We use S to denote a scalar and ψ for a fermion, subscripts are the transformation properties (or charge) under the SM group in the order $SU(3)_c \times SU(2)_L \times U(1)_Y$. For $SU(5)$ multiplets we add a subscript "F" for fermions, no subscript for scalars.

GCU [for an early reference with new states at TeV, see [16]; for an early reference with a left-right symmetric intermediate stage at $(10^{10}$–$10^{11})$ GeV see [17]]. For a discussion of GCU in nonsupersymmetric $SU(5)$-based models see also [18,19].

In this paper we show that nonminimal $SU(5)$-based extensions of the SM can lead to good GCU, provided some beyond-SM (colored) multiplets are accidentally light. The very same TeV-scale remnants of these nonminimal models, responsible for GCU, could be (some of) the mediators of the short-range double beta decay amplitude, leading to lepton number violation (LNV) at the electroweak scale. We call this "$SU(5)$-inspired" double beta decay. Different models realizing this idea can be constructed. Since short-range diagrams for $0\nu\beta\beta$ decay always fall into one of only two possible tree-level topologies [5], we will discuss two particular variants, namely one model for topology I (T-I) and one for topology II (T-II).

The main motivation to study these $SU(5)$-inspired models is that they are experimentally falsifiable at the LHC and, possibly, in upcoming lepton flavor violation searches in the following sense. First, current limits on the half-lives of $0\nu\beta\beta$ decay in ^{76}Ge [20] and ^{136}Xe [21–23] are of the order of $(1$–$2)\times 10^{25}$ years, resulting in lower limits on the effective mass scale of the underlying operator in the range of $M_{\rm eff} \simeq (2\text{-}2.5) g_{\rm eff}^{4/5}$ TeV for our two example models, while an observation with a half-life below roughly 10^{27} years implies $M_{\rm eff} \lesssim (3$–$3.8) g_{\rm eff}^{4/5}$ TeV. Here, $g_{\rm eff}$ is the mean of the couplings entering in the $0\nu\beta\beta$ decay diagram(s), see below, with $g_{\rm eff}$ required to be roughly of the order $\mathcal{O}(0.1$–$1)$ to give an observable decay rate. Negative searches at the LHC in run II will allow the covering of this range of masses [3,4]. Second, oscillation experiments have shown[3] that lepton flavor is violated (LFV). If our models are to explain neutrino data consistently, LFV violating entries in the Yukawa couplings are therefore required. These will lead to nonzero rates in processes such as $\mu \to e\gamma$, with expected rates that could be of the order of the current experimental limit [25].

We should also add a disclaimer about naturalness here. Standard $SU(5)$ suffers from what is known as the doublet-triplet splitting problem, i.e., the fact that the SM Higgs has a mass of $m_h \simeq 125$ GeV [26,27] while the colored triplet in the **5** must have a grand unified theory (GUT) scale mass. Although several solutions to this problem have been suggested (for a short review see [28]), we do not concern ourselves with any particular one. Instead, we view this simply as a fine-tuning problem and, in fact, to make the exotic particles in our models light will require, in general, additional fine-tunings. We assured ourselves, however, that this can be done consistently for all the light states (details can be found in Appendix B).

[3]See for example the recent fit [24].

The rest of this paper is organized as follows. In Sec. II we discuss our model based on topology I. It has three new multiplets when compared to minimal $SU(5)$, one of which could contain a good candidate for the cold dark matter in the Universe. The model also has a colored octet fermion and a scalar leptoquark at the TeV scale, both of which can be produced at the LHC. Neutrino masses are dominated by two-loop diagrams. Section III discusses the model based on T-II. More light states exist in this variant model, leading to a more diverse phenomenology. As in model T-I, in model T-II neutrino masses are generated at two-loop order. There are new colored sextets, which have particularly large LHC cross sections, and there is also a doubly charged scalar. We then close the paper with a short conclusion. Many of the technical aspects of our work are deferred to Appendixes A–C, where we give details of the Lagrangians of the two models, discuss briefly some aspects of fine-tuning in $SU(5)$ and present a table with the decompositions of larger $SU(5)$ multiplets.

II. A SIMPLE MODEL WITH A SCALAR QUADRUPLET

We start this section with some preliminary comments. Minimal $SU(5)$ puts the three standard model families of fermions into three copies of $\bar{\mathbf{5}}_F$ and $\mathbf{10}_F$. To generate the SM Dirac masses at least one scalar **5** is needed. Although not strictly speaking "minimal" we allow, in principle, also for the presence of a scalar **45** at the GUT scale. This **45** is added for the sole purpose of generating a Georgi-Jarlskog factor for fermion masses [29]—see Appendix B. In addition, at least one scalar **24** is needed to break $SU(5)$ to the SM group. As mentioned already in the introduction, the Lagrangian of this minimal model conserves $B-L$ [6].

Both our models need to introduce larger representations. For completeness we give in Appendix C the decomposition into SM group representations of all $SU(5)$ multiplets up to the **75**. Once these larger multiplets are added, $B-L$ will be violated, as discussed with the example of the **15** in the introduction.

Let us now turn to our first example model, which we call T-I in the following. To generate a topology I $0\nu\beta\beta$ decay, an exotic fermion is needed. We thus add to minimal $SU(5)$ three multiplets: two scalars (**15** and **70**) and one fermion ($\mathbf{24}_F$). The **15** and $\mathbf{24}_F$ will generate $0\nu\beta\beta$ decay and neutrino masses, while the **70** can play the role of a dark matter candidate, as explained later on. Details of the Lagrangian of the model are given in Appendix B. Here we only discuss the most relevant terms. Consider first the interaction among the **15**, the $\mathbf{24}_F$ and the SM fermions:

$$\mathcal{L} = \hat{y}_{ij}^{(5)} \bar{\mathbf{5}}_{F,i} \bar{\mathbf{5}}_{F,j} \mathbf{15} + \hat{y}_{i}^{(7)} \mathbf{10}_{F,i} \mathbf{24}_F \mathbf{15}^* + \cdots . \quad (1)$$

If we add to Eq. (1) a Majorana mass term for the $\mathbf{24}_F$,

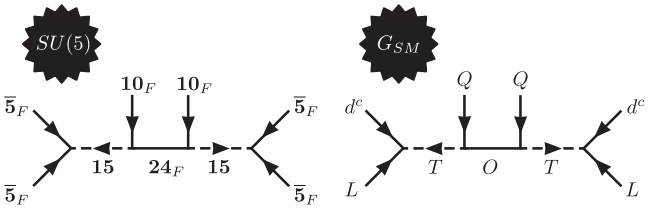

FIG. 1. Double beta decay short-range diagram in $SU(5)$ language (left) and in the $G_{\rm SM}$ language (right). The fields $\bar{\mathbf{5}}_F$ and $\mathbf{10}_F$ contain the standard model fermions, while $\boldsymbol{T} = S_{\mathbf{3},\mathbf{2},1/6}$ and $\boldsymbol{O} = \psi_{\mathbf{8},\mathbf{1},0}$ are the light pieces coming from the $\mathbf{15}$ and $\mathbf{24}_F$, respectively.

$$\mathcal{L}^M = m_{\mathbf{24}}\mathbf{24}_F\mathbf{24}_F, \tag{2}$$

an effective $d = 9$ operator is generated, which in $SU(5)$ language reads

$$\mathcal{O}_9 \propto (\bar{\mathbf{5}}_F\bar{\mathbf{5}}_F)(\mathbf{10}_F)(\mathbf{10}_F)(\bar{\mathbf{5}}_F\bar{\mathbf{5}}_F) \tag{3}$$

—see the left-hand side of Fig. 1. Under the SM group, the $\mathbf{15}$ and the $\mathbf{24}_F$ break as $S_{\mathbf{3},\mathbf{2},1/6} + \cdots \equiv \boldsymbol{T} + \cdots$ and $\psi_{\mathbf{8},\mathbf{1},0} + \cdots \equiv \boldsymbol{O} + \cdots$, respectively. The above Lagrangian equations (1) and (2) then contain the following terms:

$$\mathcal{L} = y^{(4)}_{ij} L_i d^c_j \boldsymbol{T} + y^{(5)}_i Q_i \boldsymbol{O}\boldsymbol{T}^* + m_O \boldsymbol{O}\boldsymbol{O}, \tag{4}$$

with $y^{(4)} = \hat{y}^{(5)}$, $y^{(5)} = \hat{y}^{(7)}$ and $m_O = m_{\mathbf{24}}$ in the $SU(5)$ symmetric phase.

Equation (4) will produce an operator that generates a contribution to double beta decay via

$$\mathcal{O}^{4-i}_{11} \propto (Ld^c)(Q)(Q)(Ld^c). \tag{5}$$

Here, the subscript "11" indicates the number of this $\Delta L = 2$ operator in the list defined by Babu and Leung [30], while the superscript "$4 - i$" identifies the double beta decay decomposition according to the list of [5]. The diagram which generates this operator is shown in Fig. 1, on the right. In order for this diagram to give a sizable contribution to the total $0\nu\beta\beta$ decay amplitude, $\boldsymbol{T}$ and $\boldsymbol{O}$ must have masses of the TeV order. The amplitude for this diagram has been calculated in [5]: the limit from ^{136}Xe [21–23] results in $M_{\rm eff} \gtrsim 2.5 g^{4/5}_{\rm eff}$ TeV, where $M_{\rm eff} = (m^4_T m_O)^{1/5}$ and $g_{\rm eff}$ is the (geometric) mean of the four couplings entering the diagram. In addition to this diagram, $0\nu\beta\beta$ decay will receive also a contribution from the mass mechanism. We will compare the short-range contribution and mass mechanism below, when discussing neutrino masses in this model.

We now turn to the discussion of the $\mathbf{70}$ scalar representation. The standard model does not contain a particle candidate for the cold dark matter (DM). It is, however, quite straightforward to identify the basic requirements for SM multiplets to contain viable dark matter candidates. As shown in Table I in the Appendix C, the $\mathbf{70}$ is one of the smallest $SU(5)$ multiplet containing an $SU(2)_L$ quadruplet, $\mathbf{70} = S_{\mathbf{1},\mathbf{4},1/2} + \cdots \equiv \boldsymbol{K} + \cdots$. $S_{\mathbf{1},\mathbf{4},1/2}$ contains one electrically neutral state, $\boldsymbol{K}^0$, which after the breaking of $SU(2)_L$ can play the role of the cold dark matter.

Of course, only particles stable over cosmologically long times can be dark matter. In the $SU(5)$ phase, model T-I allows, in principle, a quartic scalar term $\mathbf{5}\cdot\mathbf{5}\cdot\mathbf{5}^*\cdot\mathbf{70}^*$ which could induce the decay $\boldsymbol{K}^0 \to hhh$. To eliminate this coupling, and all other couplings linear or cubic in $\mathbf{70}$, one has to postulate a Z_2 symmetry. We simply assume $\boldsymbol{K}$ to be odd under this Z_2,[4] while all other particles of the model are even. We will not discuss further details of the phenomenology of $\boldsymbol{K}^0$ as a DM candidate; these have been worked out in [31]. Note that according to [31], the neutral member of $\boldsymbol{K}$ can play the role of DM if $m_{K^0} \simeq 2.4$ TeV.

Adding complete $SU(5)$ multiplets to the SM does not change GCU, since the β coefficients of all three gauge couplings change by the same amount. However, after $SU(5)$ breaking, the masses of the different $G_{\rm SM}$ multiplets contained within each $SU(5)$ representation may be different, yielding a large number of possibilities to achieve GCU.

The β coefficients for the running of the gauge couplings,[5] including the contributions from $\boldsymbol{T}$, $\boldsymbol{O}$ and $\boldsymbol{K}$, are

$$b_i = \begin{pmatrix} \frac{13}{3} \\ -1 \\ \frac{-14}{3} \end{pmatrix}, \qquad b_{ij} = \begin{pmatrix} \frac{326}{75} & 12 & \frac{28}{3} \\ 4 & 94 & 20 \\ \frac{7}{6} & \frac{15}{2} & \frac{88}{3} \end{pmatrix}, \tag{6}$$

at one-loop and two-loop order, respectively. Figure 2 shows the resulting running of the inverse gauge couplings as a function of energy, assuming that the masses of $\boldsymbol{T}$, $\boldsymbol{O}$ and $\boldsymbol{K}$ are of the TeV order. Here, we neglect the small two-loop contributions from Yukawa couplings for simplicity, and we also do not consider possible corrections from GUT-scale thresholds.

As Fig. 2 shows, the model nicely unifies with an estimated GUT scale of $m_G \simeq 10^{17}$ GeV, which gives an estimated half-life for gauge-mediated proton decay of $T_{1/2}(p) \sim 10^{38}$ y, albeit with a large uncertainty. Recall that the current constraint from Super-Kamiokande is $\tau_{p\to\pi^0 e^+} \gtrsim 10^{34}$ y [32].

However, while the model is automatically safe from the gauge-mediated proton decay diagrams, we have to impose one more constraint on the model, due to scalar-mediated proton decay. The triple-scalar term $\mathbf{5}\cdot\mathbf{5}\cdot\mathbf{15}^*$, see Fig. 3,

[4]A nonzero vacuum expectation value (VEV) of the $\boldsymbol{K}^0$ would break this Z_2 spontaneously and, thus, has to be avoided. For $m^2_K > 0$ one expects a zero VEV to be the preferred solution of the tadpole equations.

[5]In general, ignoring the effect of Yukawa interactions, the running gauge couplings g_i change with the logarithm of the energy scale $t \equiv \log E$ as follows: $dg_i/dt = b_i g_i^3/(4\pi)^2 + b_{ij} g_i^3 g_j^2/(4\pi)^4$.

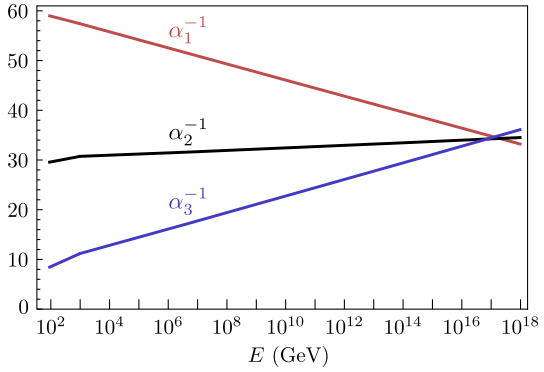

FIG. 2 (color online). Gauge coupling unification in model T-I. In this calculation the new states are assumed to have masses around $M \sim \mathcal{O}(1)$ TeV. The running includes two-loop β coefficients but does not consider any GUT-scale thresholds.

leads to a vertex $S_{\mathbf{3},\mathbf{1},-1/3}\boldsymbol{HT}$. After electroweak symmetry breaking this can be considered as an effective mixing of $\boldsymbol{T}$ with the colored triplet $S_{\mathbf{3},\mathbf{1},-1/3}$. Note, however, that in the full model there is more than one contribution to this vertex, since the field content of the model also allows the writing of the interaction $\mathbf{5}\cdot\mathbf{5}\cdot\mathbf{15}^*\cdot\mathbf{24}$. Furthermore, there is a second $S_{\mathbf{3},\mathbf{1},-1/3}$ inside the **45** which needs to be taken into consideration. As such, if we call μ_1 and μ_2 the effective interactions of these two heavy colored scalars (assumed to have a degenerate mass of the order of the GUT-scale m_G) with H and $\boldsymbol{T}$, then

$$\mu_1 = 2\cos\alpha\hat{h}_{\mathbf{5}\cdot\mathbf{5}\cdot\mathbf{15}^*} + 2\cos\alpha\hat{\lambda}_{\mathbf{5}\cdot\mathbf{5}\cdot\mathbf{15}^*\cdot\mathbf{24}}\langle\mathbf{24}\rangle - \sin\alpha\sum_{a=1,2}\hat{\lambda}_{[\mathbf{5}\cdot\mathbf{45}\cdot\mathbf{15}^*\cdot\mathbf{24}]_a}\langle\mathbf{24}\rangle, \tag{7}$$

$$\mu_2 = \cos\alpha\sum_{a=1,2}\hat{\lambda}_{[\mathbf{5}\cdot\mathbf{45}\cdot\mathbf{15}^*\cdot\mathbf{24}]_a}\langle\mathbf{24}\rangle - 2\sin\alpha\left(\hat{h}_{\mathbf{45}\cdot\mathbf{45}\cdot\mathbf{15}^*} + \sum_{a=1,2}\hat{\lambda}_{[\mathbf{45}\cdot\mathbf{45}\cdot\mathbf{15}^*\cdot\mathbf{24}]_a}\langle\mathbf{24}\rangle\right), \tag{8}$$

where α is the angle controlling the admixture of the $S_{\mathbf{1},\mathbf{2},1/2}$ representations in the **5** and **45** forming the light state H, $\hat{h}$ ($\hat{\lambda}$) represent the trilinear (quartic) scalar couplings of the

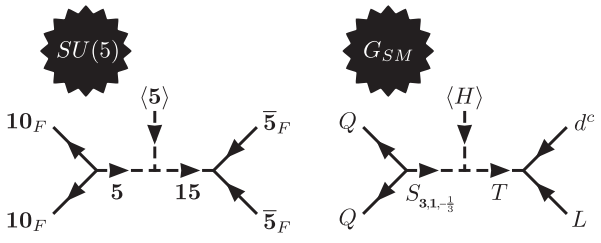

FIG. 3. Scalar-mediated proton decay in model T-I. Mixing induced via the SM Higgs VEV between $\mathbf{S_{1,3,-1/3}}$ and $\boldsymbol{T}$ can generate an effective diquark coupling for $\boldsymbol{T}$.

$SU(5)$ fields indicated in subscript, and the index a keeps track of the different gauge invariant contractions of the representations. The VEV of the **24** must be in the SM-singlet direction.

Since the $S_{\mathbf{3},\mathbf{1},-1/3}$ fields has diquark couplings, a proton decay diagram is induced by this $S_{\mathbf{3},\mathbf{1},-1/3} \leftrightarrow \boldsymbol{T}$ mixing. Consistency with proton decay limits can be converted into an upper limit on the sum of the two μ_i couplings, $\mu \equiv \mu_1 + \mu_2$, which is, very roughly, of the order of

$$\frac{\mu}{m_G} \lesssim 2.5\times 10^{-6}\left(\frac{0.1}{y_{11}^{(4)}}\right)\left(\frac{2\text{ TeV}}{m_T}\right)^2. \tag{9}$$

Here we assume that the typical value of $y_{11}^{(4)}$ is $\mathcal{O}(0.1)$. Much smaller values, say $y_{11}^{(4)} \simeq y_e$, would avoid the fine-tuning of Eq. (9), but at the same time they would render the $0\nu\beta\beta$ diagram in Fig. 1 unobservable.

We note that a very similar discussion about scalar-mediated proton decay can be found in [18,33]. Reference [18] considers also $SU(5)$, while [33] discusses an $SO(10)$-based model. In [33], however, the authors argue against the existence of light color-triplet scalars on the basis of this constraint, while we accept Eq. (9) as just one (more) fine-tuning.

Let us now discuss neutrino masses. The **15** also contains the $S_{\mathbf{1},\mathbf{3},1}$, which is often denoted as Δ in neutrino physics [34,35]. Thus, after integrating out the heavy Δ, effectively a Weinberg operator [36] is generated. After the breaking of $SU(2)_L$, one thus finds a type-II seesaw contribution to the neutrino mass. One can estimate this contribution to be of the order of

$$(m_\nu)_{ij} \simeq \hat{y}_{ij}^{(5)} v_{\text{SM}}^2 \frac{\mu_\Delta}{m_\Delta^2} \sim 0.3\text{ meV}. \tag{10}$$

For $\hat{y}_{ij}^{(5)} = 1$ and $\mu_\Delta = m_\Delta \simeq m_G$, with a GUT scale of, see Fig. 2, $m_G \simeq 10^{17}$ GeV. This is too small to explain solar neutrino oscillations by a factor of roughly 30.

Note that the effective μ_Δ contains contributions from the same couplings ($\mathbf{5}\cdot\mathbf{5}\cdot\mathbf{15}^*$, etc.) as discussed just above for the scalar-induced proton decay. The different $SU(5)$ terms contribute, however, with different Clebsch-Gordon coefficients to μ_Δ than those appearing in μ; see again Appendix B for details. Thus, μ and μ_Δ can easily take very different values. Of course, if μ_Δ were to obey a limit similar to Eq. (9), contributions to neutrino masses would actually be much smaller than the numerical value in Eq. (10).

The failure to have a sufficiently large neutrino mass to explain solar and atmospheric data via the type-II seesaw contribution[6] does not imply that the model cannot explain neutrino oscillation data. This is due to the two-loop

[6]Unless m_Δ is tuned to be much smaller than the GUT scale, which would harm the successful GCU.

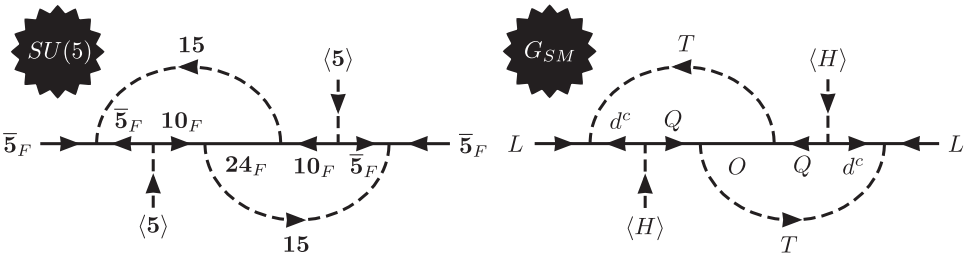

FIG. 4. Two-loop neutrino mass diagram in model T-I. To the left, the $SU(5)$ origin of the diagram; to the right the contributions to m_ν from the light states of the model.

contribution to the neutrino mass matrix, involving the leptoquark and the colored fermion, shown in Fig. 4 (on the right). The left diagram shows the $SU(5)$ origin of this diagram; the diagram to the right is in the SM phase.

Using the general analysis of two-loop diagrams of [37] one can calculate the contribution of this diagram to the neutrino mass matrix. However, since a two-loop model based on this diagram has been discussed recently in [38], we will not repeat all the details here and show only a few rough estimates. For $m_T \simeq m_O \gg m_b$ Fig. 4 gives approximately

$$(m_\nu)_{ij} \simeq \frac{N_c}{(16\pi^2)^2}\frac{1}{\Lambda_{\rm LNV}}(m_{d_k} m_{d_m} y^{(4)}_{ik} y^{(4)}_{jm} y^{(5)}_k y^{(5)}_m + (i \leftrightarrow j)). \tag{11}$$

N_c is a color factor ($N_c = 3$ for this diagram) and logarithmic terms from the loop integrals have been neglected for simplicity. $\Lambda_{\rm LNV}$ is the mean of the masses of $m_T \simeq m_O$. Note that Eq. (11) produces three nonzero neutrino masses, which in leading order will be proportional to $m_{\nu_{1,2,3}} \propto m_b m_d, m_b m_s, m_b^2$. While it is possible to fit quasi-degenerate neutrino masses with Eq. (11), the hierarchy in down quark masses leads us to expect that neutrino masses follow a normal hierarchical neutrino spectrum in model T-I. For $\Lambda_{\rm LNV} \simeq 1$ TeV, $|y^{(4)}_3| \sim y^{(5)}_3 \simeq 0.06$ and $|y^{(4)}_2| \sim y^{(5)}_2 \simeq 0.26$, where $|y^{(4)}_k| = \sqrt{\sum_j (y^{(4)}_{jk})^2}$, one obtains $m_{\nu_{2,3}} \simeq (9\times 10^{-3}, 5\times 10^{-2})$ eV, correctly reproducing the atmospheric and solar neutrino mass scales (for normal hierarchy).

With two Yukawa vectors ($y^{(4)}_{i3}$ and $y^{(4)}_{i2}$) contributing (dominantly) to the flavor structure of $(m_\nu)_{ij}$, there are four independent ratios, which we arbitrarily choose to be $(y^{(4)}_{13}/y^{(4)}_{33}, y^{(4)}_{23}/y^{(4)}_{33})$ and $(y^{(4)}_{12}/y^{(4)}_{32}, y^{(4)}_{22}/y^{(4)}_{32})$. With these we can easily fit the observed neutrino angles. Many solutions exist and can be found in a simple numerical scan. We only quote one particular example as a proof of principle. Choosing the absolute values of the Yukawa couplings as mentioned above, $(y^{(4)}_{13}/y^{(4)}_{33}, y^{(4)}_{23}/y^{(4)}_{33}) \sim (0.03, -1.7)$ and $(y^{(4)}_{12}/y^{(4)}_{32}, y^{(4)}_{22}/y^{(4)}_{32}) \sim (1, 1)$ gives all three measured neutrino angles near their best fit points [24]. Nevertheless, we stress again that these numerical examples give only a rough estimate.

One should also compare the size of the relative contributions to the $0\nu\beta\beta$ decay rate of the short-range diagram (see Fig. 1) with the one of the neutrino mass mechanism [39]. The current limits on $0\nu\beta\beta$ decay from ^{76}Ge and ^{136}Xe correspond to an upper limit on the effective neutrino mass, $\langle m_\nu\rangle$, of roughly $\langle m_\nu\rangle \lesssim (0.2\text{–}0.4)$ eV, depending on the choice of nuclear matrix elements [40–42]. Experiments on these nuclei with a sensitivity of 10^{27} years would probe $\langle m_\nu\rangle \simeq 50$ meV. For a normal hierarchical neutrino mass spectrum, as in our example fit discussed above, much larger half-lives are expected. The short-range diagram gives a half-life of roughly 10^{27} years for $M_{\rm eff} \gtrsim g_{\rm eff}^{4/5}$ TeV, corresponding to $M_{\rm eff} \gtrsim 1.7$ TeV for $g_{\rm eff} = \sqrt{y^{(4)}_{11} y^{(5)}_1} \simeq 0.35$. The latter can be completely covered by LHC searches for the signal $l^+l^+ + 4j$, as discussed below.

We have also estimated $\mathrm{Br}(\mu \to e\gamma)$ for this model. Using the formulas [38,39] we can roughly estimate $\mathrm{Br}(\mu \to e\gamma) \simeq 3\times 10^{-13} |y^{(4)}_{13} y^{(4)*}_{23}|^2$ for a leptoquark mass of $M_O \simeq 1$ TeV. This is roughly of the order of the limit expected for the second phase of the MEG experiment [25]. A much more detailed discussion about LFV can be found in [38].

We now discuss briefly LHC searches for model T-I. Leptoquarks have been searched at the LHC in run I by both the ATLAS [43,44] and the CMS [45–47] Collaborations. No positive observation of any leptoquark (LQ) state has been reported, apart from a possible 2.6σ excess near $m_{\rm LQ} \simeq 650$ GeV found in [45]. Lower limits on LQ masses depend on the lepton generation they couple to, and on the branching ratios of the LQs. Lower limits are roughly 650–1000 GeV [43–47] for searches based on some pair-produced LQs, depending on assumptions. We also mention the recent CMS search for singly produced LQ states. This search excludes single production of first generation LQs with masses below 1730 GeV (895 GeV) for leptoquark couplings equal to $y = 1$ ($y = 0.4$) [48]. Run II will improve these numbers in the very near future.

The colored fermionic octet $\boldsymbol{O}$ can be pair produced at the LHC in gluon-gluon fusion. We have implemented the model in SARAH [49,50] and used the TOOLBOX environment [51] to generate SPHENO [52,53] and MADGRAPH files. We then used MADGRAPH5 [54] for a quick estimation of the cross section for pair producing $\boldsymbol{O}$ at $\sqrt{s} = 8$ and $\sqrt{s} = 13$ TeV. The kinematics of this decay depends on the mass hierarchy between $\boldsymbol{O}$ and our leptoquark $\boldsymbol{T}$, but the decays of $\boldsymbol{O}$ will always lead to a final state containing two hard jets plus a charged lepton or neutrino (i.e., missing E_T). In total, the signal will thus consist of four hard jets with 2,1 or 0 charged leptons. Because of the Majorana nature of $\boldsymbol{O}$, the ratio $\boldsymbol{R}$ of the number of same-sign to opposite-sign charged lepton events is expected to be $R = 1$.

Also, we expect that the signal will contain lepton flavor violating events, i.e., final states $e^+\mu^+$ plus jets (and also events with taus). This is caused by the flavor structure of the leptoquark couplings $y^{(4)}_{ik}$, which is needed to explain neutrino angles and which enter in the decay rate of the state $\boldsymbol{O}$.

While there is no dedicated search for this signal at either CMS or ATLAS, we can use the results of the CMS search for right-handed neutrinos in left-right symmetric models [55] to estimate roughly the current sensitivity of LHC to $\boldsymbol{O}$. The CMS Collaboration uses the final state $2l + 2j$ to extract lower limits on the masses of W_R and ν_R, but it mentions explicitly that in the final state they allow for any number of jets larger or equal to two.[7] Below $m_{lljj} \sim 2$ TeV the limits derived by CMS are background dominated. Since one can expect that backgrounds are smaller for signals with a larger number of jets, we can thus use the derived upper limits on $\sigma(pp \to lljj)$ to conservatively estimate lower limits on m_O. Unfortunately, CMS decided to show limits only for $m_{lljj} \geq 1$ TeV, with upper limits on $\sigma(pp \to eejj)$ and $\sigma(pp \to \mu\mu jj)$ both of the order of $\sim$9 fb for this lowest mass (summed over both lepton charges). Comparing with their Fig. 2 [55], one can estimate that in the bins [0.8, 1] ([0.6, 0.8]) TeV upper limits should be roughly 14 (23) fb. Comparing with the calculated $\sigma(pp \to \boldsymbol{OO})$ of 24 (64) fb for $m_O =$ 900 (800) GeV and assuming a branching ratio $\mathrm{Br}(\boldsymbol{OO} \to ll + 4j) \simeq 25\%$, we estimate that the current lower limit on m_O should be roughly in the 800–900 GeV ballpark. More exact numbers would require a dedicated search by the experimental collaborations. However, for $\sqrt{s} = 13$ TeV, cross sections will be much larger and we estimate a dedicated search could be sensitive up to $m_O \simeq$ (2.1–2.2) TeV with $\mathcal{L} \simeq 300$ fb^{-1}, corresponding to (16–10) events before cuts.

[7]There is a 2.8σ excess in the data at $m_{eejj} \simeq 2.2$ TeV, but CMS concludes that it is not in agreement with expectations for a left-right symmetric model. Our model T-I cannot explain this excess either.

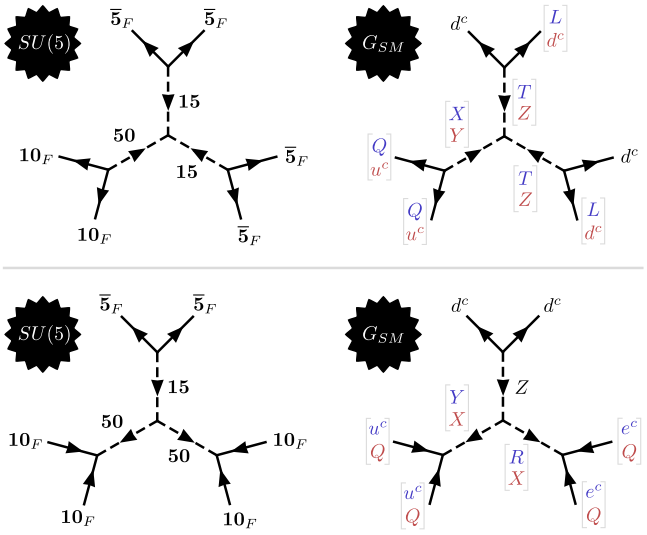

FIG. 5 (color online). Dimension-9 operators in model T-II built with $SU(5)$ representations (left) and with the corresponding light $G_{\rm SM}$ pieces (right). Here, in addition to $\boldsymbol{T} \equiv S_{\boldsymbol{3},\boldsymbol{2},1/6}$, we are using the shorthand notation $\boldsymbol{R} = S_{\boldsymbol{1},\boldsymbol{1},-2}$, $\boldsymbol{X} = S_{\boldsymbol{6},\boldsymbol{3},-1/3}$, $\boldsymbol{Y} = S_{\bar{\boldsymbol{6}},1,4/3}$ and $\boldsymbol{Z} = S_{\bar{\boldsymbol{6}},1,-2/3}$. These operators generate $0\nu\beta\beta$ decay [with the blue (top) fields on the right diagrams] as well as $n - \bar{n}$ oscillations [with the red (bottom) fields]—see text for a discussion.

III. MODEL T-II: ADDING COLORED SEXTETS

Topology II for $0\nu\beta\beta$ decay consists of diagrams in which three scalars are interchanged between the six SM fermions that make up the $0\nu\beta\beta$ decay operator [5]. For model T-II we therefore add two copies of the scalar **15** plus one scalar **50** to minimal $SU(5)$. The Lagrangian of the model is given in the Appendix A. Here we discuss only the most relevant terms. In the $SU(5)$ phase the Lagrangian includes

$$\mathcal{L}_{FFS} = \hat{y}^{(5)}_{ijk}\bar{\mathbf{5}}_{F,i}\bar{\mathbf{5}}_{F,j}\mathbf{15}_k + \hat{y}^{(6)}_{ij}\mathbf{10}_{F,i}\mathbf{10}_{F,j}\mathbf{50} + \cdots, \quad (12)$$

$$\mathcal{L}_{SSS} = \hat{h}^{(2)}_{ij}\mathbf{15}_i\mathbf{15}_j\mathbf{50} + \hat{h}^{(3)}_{i}\mathbf{15}_i\mathbf{50}^*\mathbf{50}^* + \cdots, \quad (13)$$

where the dots stand for additional terms. Terms in Eq. (12), together with the corresponding mass terms for **15** and **50**, produce the $d = 9$ operators shown in Fig. 5 on the left.

We introduce the shorthand notation

$$\boldsymbol{T} \equiv \left(\mathbf{3}, \mathbf{2}, \frac{1}{6}\right), \qquad \boldsymbol{Z} \equiv \left(\mathbf{6}, \mathbf{1}, -\frac{2}{3}\right) \in \mathbf{15}, \quad (14)$$

$$\boldsymbol{R} \equiv (\mathbf{1}, \mathbf{1}, -2), \quad \boldsymbol{X} \equiv \left(\bar{\mathbf{6}}, \mathbf{3}, -\frac{1}{3}\right), \quad \boldsymbol{Y} \equiv \left(\mathbf{6}, \mathbf{1}, \frac{4}{3}\right) \in \mathbf{50}. \quad (15)$$

Differently from model T-I, we will assume that there are a total of six light states: two copies of $\boldsymbol{T}$ plus one copy of $\boldsymbol{R}$, $\boldsymbol{X}$, $\boldsymbol{Y}$ and $\boldsymbol{Z}$. The Lagrangian in the SM phase then contains the following terms:

$$\mathcal{L}_{FFS} = y^{(4)}_{ijk} L_i d^c_j \boldsymbol{T}_k + y^{(5)}_{ij} d^c_i d^c_j \boldsymbol{Z} + y^{(6)}_{ij} e^c_i e^c_j \boldsymbol{R} + y^{(7)}_{ij} Q_i Q_j \boldsymbol{X} + y^{(8)}_{ij} u^c_i u^c_j \boldsymbol{Y} + \text{H.c.}, \quad (16)$$

$$\mathcal{L}_{SSS} = h^{(1)}_{ij} \boldsymbol{T}_i \boldsymbol{T}_j \boldsymbol{X} + h^{(2)} \boldsymbol{Y}\boldsymbol{Z}\boldsymbol{Z} + h^{(3)} \boldsymbol{R}^* \boldsymbol{Y}^* \boldsymbol{Z} + h^{(4)} \boldsymbol{X}^* \boldsymbol{X}^* \boldsymbol{Z} + \text{H.c.} \quad (17)$$

With these terms the diagrams in the left of Fig. 5 produce two diagrams each in the SM phase of the model. These are shown in Fig. 5 on the right. We stress again that the central couplings in these diagrams, proportional to the couplings $h^{(1)} - h^{(4)}$, receive contributions from several terms of the Lagrangian in the $SU(5)$ phase of the model and, as discussed in the Appendixes A and B, can therefore take quite different values, despite their common origin.

Consider first the diagrams on the right-hand side of Fig. 5 containing two external leptons. We can easily identify them with the T-II operators classified in [5] as

$$\mathcal{O}^{\text{T-II}-4}_{11} = (\bar{L}\bar{d}^c)(\bar{L}\bar{d}^c)(\bar{Q}\,\bar{Q}), \quad (18)$$

$$\mathcal{O}^{\text{T-II}-3}_{-} = (e^c e^c)(\bar{d}^c \bar{d}^c)(u^c u^c). \quad (19)$$

Here, again the subscript "11" identifies the Babu and Leung operator [30], whereas "–" is the missing $\Delta L = 2$ dimension-9 operator in this list. The superscripts indicate the $0\nu\beta\beta$ decay label in the classification scheme of [5]. The latter allows us to estimate the $0\nu\beta\beta$ decay rates induced by these two diagrams. By coincidence the two operators give very similar limits: using again the experimental limits from [21–23] results in $M_{\text{eff}} \gtrsim 2.2 g^{4/5}_{\text{eff}}$ TeV for each of the two operators. As before, M_{eff} stands for the mean of the masses entering the diagram and for the definition of the mean coupling g_{eff} we have made $h^{(1)}$ and $h^{(3)}$ dimensionless by introducing $g^{(k)} \equiv h^{(k)}/M_{\text{eff}}$. We stress that, in contrast to model T-I, here all light states appear in at least one tree-level double beta decay diagram. However, this variant model does not include a dark matter candidate.

The two diagrams on the right-hand side of Fig. 5 also produce the operators

$$\mathcal{O}_{\Delta B=2,\Delta L=0} = (\bar{d}^c \bar{d}^c)(\bar{d}^c \bar{d}^c)(\bar{u}^c \bar{u}^c), \quad (20)$$

$$\mathcal{O}_{\Delta B=2,\Delta L=0} = (QQ)(\bar{d}^c \bar{d}^c)(QQ). \quad (21)$$

Both of these operators induce $n - \bar{n}$ oscillations—see for example the review [56]. The current limit on the lifetime of neutron-antineutron oscillations is $\tau_{n\to\bar{n}} > 0.86 \times 10^8$ s [57] and, as discussed in that paper, one expects an improvement on this number of about 2 orders of magnitude in the future. We can estimate the lifetime of neutron-antineutrino oscillations, $\tau_{n-\bar{n}}$, adapting the formulas from [33] for our model. Introducing the notation $\bar{g} = (y^{(7)}_{11})^{2/3}(y^{(5)}_{11})^{1/3}$, one gets from the current experimental limit a constraint

$$h^{(4)} \lesssim 0.6 \times 10^{-6} \left(\frac{0.1}{\bar{g}}\right)^3 \left(\frac{M_{\text{eff}}}{3\ \text{TeV}}\right)^6 \text{GeV} \quad (22)$$

for the bottom right diagram in Fig. 5 [in this case, $M_{\text{eff}} = (m^4_X m^2_Z)^{1/6}$]. The same constraint applies to $h^{(2)}$ from the top right diagram of Fig. 5. This fine-tuning could only be avoided if $\boldsymbol{Z}$ takes a mass of the order of the GUT scale, as in the model of [33], which would, however, destroy gauge coupling unification in model T-II discussed next.

For model T-II we find the following β coefficients:

$$b_i = \begin{pmatrix} \frac{241}{30} \\ \frac{11}{6} \\ -\frac{13}{6} \end{pmatrix}, \qquad b_{ij} = \begin{pmatrix} \frac{1691}{30} & \frac{129}{10} & \frac{1988}{15} \\ \frac{43}{10} & \frac{785}{6} & 188 \\ \frac{497}{30} & \frac{141}{2} & \frac{541}{3} \end{pmatrix}. \quad (23)$$

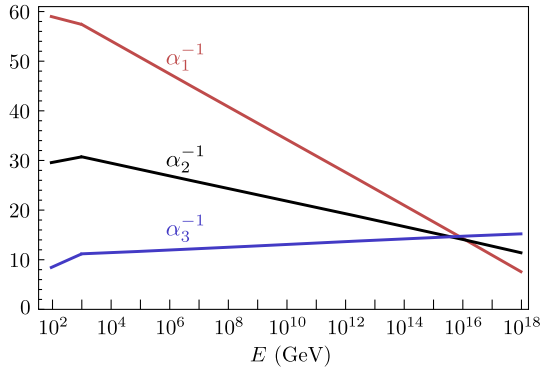

FIG. 6 (color online). Gauge coupling unification in model T-II. In this example calculation the new states are assumed to have masses around $M \sim \mathcal{O}(1)$ TeV. As in Fig. 2, the running includes two-loop β coefficients but does not consider any GUT-scale thresholds.

Figure 6 shows the corresponding running of the inverse gauge couplings for masses of the new particles $M \sim \mathcal{O}(1)$ TeV. Despite the very different particle content of model T-II, compared to model T-I, GCU works very nicely. The estimated GUT scale in this model is found to be roughly $m_G \simeq 5 \times 10^{15}$ GeV, lower than in model T-I. Also α_G is predicted to be much larger than in model T-I. This can be easily understood from the β coefficients, which are larger due to the presence of color sextets in the running.

The best-fit point for the proton decay half-life is found to be $\tau_{p\to\pi^0 e^+} \simeq 5 \times 10^{33}$ y, slightly below the current experimental limit [32]. However, it is well known that

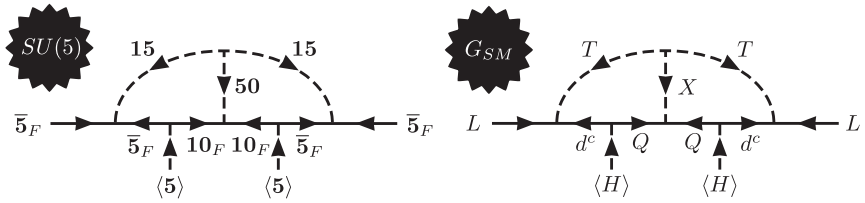

FIG. 7. Two-loop neutrino mass diagrams in model T-II. The structure is as in BZ.

predictions of proton decay half-lives have a large error bar. We have repeated the exercise of estimating the uncertainty in the GUT scale due to the neglected GUT-scale thresholds, following the χ^2 procedure of [58]. We will not show the plots corresponding to model T-II here, since the results are similar to the example models discussed in [58]. From this exercise we estimate that typical uncertainties in the predicted proton-decay half-life should be around (2–2.5) orders of magnitude. The planned Hyper-Kamiokande experiment might cover a large part of this range [59]. Note that, since model T-II has the same light leptoquark state $\boldsymbol{T}$ which appears in model T-I, the constraint on scalar-mediated proton decay, see Eq. (9), applies also in model T-II.

We now briefly discuss neutrino masses. Since the GUT scale in model T-II is expected to be lower than in model T-I, the type-II seesaw contribution could be as large as $(m_\nu)_{ij} \simeq 6 y^{(4)}_{ij}$ meV, assuming $\mu_\Delta = m_\Delta \simeq m_G$. This is, in principle, large enough to explain the solar neutrino scale. However, $\mu_\Delta \ll m_G$ and/or $y^{(4)}_{ij} < 1$ would render this contribution negligible.

More important is the radiative contribution from TeV-scale particles. The operators in Eqs. (18) and (19) will produce two-loop ($\mathcal{O}^{\text{T-II}-4}_{11}$) and four-loop ($\mathcal{O}^{\text{T-II}-3}_{-}$) neutrino masses. The contribution to the neutrino mass matrix from four-loop diagrams is expected to be at most $(m_\nu)_{\tau\tau} \sim \mathcal{O}(10^{-10})$ eV [39], so completely negligible numerically. The two-loop diagram shown in Fig. 7, on the other hand, will produce neutrino masses of the same order of Eq. (11) [37]. We do not repeat the discussion of fits to neutrino data here, since it is very similar to that of the previous subsection. Also in model T-II LFV rates are expected to be near experimental limits.

We turn now to the discussion of LHC searches. For the constraints on the leptoquark, $\boldsymbol{T}$, see the discussion for model T-I. The same constraints apply, of course, also in model T-II. Cross sections for color sextets are expected to be particularly large at the LHC [60], since they can be produced as s-channel resonances. Both ATLAS [61] and CMS [62] have searched for the appearance of new resonances in dijet spectra. Especially, [62] presents upper limits on $\sigma(pp \to jj)$ as a function of the mass of a hypothetical resonance coupled to pairs of quarks. We can combine these limits with cross section calculations for resonances coupling to uu or dd pairs; see for example [4]. We estimate that, for m_Y (m_Z) equal to 3 TeV this results in upper limits on the couplings $y^{(8)}_{11}$ ($y^{(5)}_{11}$) of roughly $y^{(8)}_{11} \lesssim 0.19$ ($y^{(5)}_{11} \lesssim 0.056$). Similar bounds can be derived for $\boldsymbol{X}$ [which nevertheless is an $SU(2)_L$ triplet, unlike $\boldsymbol{Y}$ and $\boldsymbol{Z}$]. Run II of the LHC will improve vastly on these numbers.

Much smaller couplings (and larger masses) can be probed at the LHC, if there is a certain hierarchy in masses among the states $\boldsymbol{X}$, $\boldsymbol{Y}$, $\boldsymbol{Z}$, $\boldsymbol{R}$ and $\boldsymbol{T}$. We will discuss one example. If $m_X > 2m_T$, then the diquark $\boldsymbol{X}$ will have a non-negligible decay rate to a pair of leptoquarks—see the top-right diagram in Fig. 5. The branching ratio $\text{Br}(\boldsymbol{X} \to \boldsymbol{TT})$ depends on the relative size of the couplings $h^{(1)}/m_T$ and $y^{(7)}_{ij}$. If the branching ratio is nonzero, since each of the $\boldsymbol{T}$'s will decay into $l^+ j$, the total signal is $l^+ l^+ jj$, which enjoys a background orders of magnitude lower than the dijet spectrum. Since there is little or no background in this search for large values of m_X, it might be possible to establish discovery with as few as (3–5) events.

Given that we have no theory for the couplings, $h^{(1)}/m_T$ could be much smaller than $y^{(7)}_{ij}$. However, double beta decay depends on the same couplings. Thus, a measured finite half-life in a future $0\nu\beta\beta$ decay experiment would define a lower limit on $h^{(1)}$ as a function of the mass M_{eff} in a parameter range that should be completely coverable in run II of the LHC, considering the large diquark cross sections.

Sensitivity for the doubly charged scalars at the LHC is much weaker, because of their color singlet nature. Results of searches for same-sign dilepton pairs in electron and muon final states have been published by ATLAS [63]. No deviation from SM expectations have been found and lower limits on the mass of $\boldsymbol{R}$ of roughly $m_R \gtrsim 400$ GeV are derived for $\boldsymbol{R}$ decaying to either $e^\pm e^\pm$, $e^\pm \mu^\pm$ or $\mu^\pm \mu^\pm$ with 100% branching ratio. In summary, model T-II has a particularly rich phenomenology at the LHC.

IV. CONCLUSIONS

If $B - L$ violation exists at the TeV scale, one expects also sizable contributions to the short-range part of the $0\nu\beta\beta$ decay amplitude [2,5], with interesting consequences for the viability of leptogenesis [64,65]. In this paper we have studied top-down scenarios inspired by $SU(5)$ unification. These models violate $B - L$, thus generate neutrino masses and neutrino oscillation data can be easily

fitted. As in all TeV-scale models of loop neutrino masses, one expects that charged lepton flavor violation is large and possibly within reach of near future experiments. The presence of new states at the TeV scale changes the running of the three gauge couplings in such a way that, unlike in the standard model, gauge coupling unification can be achieved without introducing supersymmetry.

We have constructed two exemplary models, one for each of the two tree-level topologies of $0\nu\beta\beta$ decay. Model T-I has a dark matter candidate and few low-scale (TeV) particles. On the other hand, there is model T-II which introduces several new scalars and thus has a richer phenomenology. The two models differ in their predicted gauge-mediated proton decay half-lives, due to their different GUT scales. Model T-II might be in reach of the planned Hyper-Kamiokande experiment [59].

The new states predicted by our models can be searched for at the LHC. We have discussed several different possible LHC searches, the most interesting of which are certainly the lepton number violating final states $l^{\pm}l^{\pm} + 2j$ and $l^{\pm}l^{\pm} + 4j$, where $l = e, \mu, \tau$. LHC can probe the part of parameter space of our models where the new states give the dominant contribution to the $0\nu\beta\beta$ decay amplitude. In this sense, our models are falsifiable experimentally. We are looking forward to the results of run II at the LHC.

ACKNOWLEDGMENTS

The authors thank S. G. Kovalenko for discussions. Work was supported by MINECO grants No. FPA2014-58183-P, Multidark No. CSD2009-00064 and the PROMETEOII/2014/084 grant from Generalitat Valenciana.

APPENDIX A: LAGRANGIANS OF THE MODELS

This Appendix contains the mass and interaction terms of the two models discussed in the main text.

1. Model T-I

Consider the usual three copies of the left-handed fermion representations $\bar{\mathbf{5}}_F$ and $\mathbf{10}_F$ of $SU(5)$ in addition to one $\mathbf{24}_F$. With an extended scalar sector consisting of one copy of the complex representations **5**, **15**, **45**, **70** and a **24** real scalar field, the allowed mass and interaction terms are the following:

$$\hat{\mathcal{L}}_{\rm int} = \hat{\mathcal{L}}_{FF} + \hat{\mathcal{L}}_{FFS} + \hat{\mathcal{L}}_{SS} + \hat{\mathcal{L}}_{SSS} + \hat{\mathcal{L}}_{SSSS}, \quad \text{(A1)}$$

$$\hat{\mathcal{L}}_{FF} = m_{\mathbf{24}}\mathbf{24}_F\mathbf{24}_F + \text{H.c.}, \quad \text{(A2)}$$

$$\begin{aligned}\hat{\mathcal{L}}_{FFS} = {}& \hat{y}^{(1)}_{ij}\bar{\mathbf{5}}_{F,i}\mathbf{10}_{F,j}\mathbf{5}^* + \hat{y}^{(2)}_{ij}\mathbf{10}_{F,i}\mathbf{10}_{F,j}\mathbf{5} + \hat{y}^{(3)}_{ij}\bar{\mathbf{5}}_{F,i}\mathbf{10}_{F,j}\mathbf{45}^* + \hat{y}^{(4)}_{ij}\mathbf{10}_{F,i}\mathbf{10}_{F,j}\mathbf{45} \\ & + \hat{y}^{(5)}_{ij}\bar{\mathbf{5}}_{F,i}\bar{\mathbf{5}}_{F,j}\mathbf{15} + \hat{y}^{(6)}_{i}\bar{\mathbf{5}}_{F,i}\mathbf{24}_F\mathbf{5} + \hat{y}^{(7)}_{i}\mathbf{10}_{F,i}\mathbf{24}_F\mathbf{15}^* + \hat{y}^{(8)}_{i}\bar{\mathbf{5}}_{F,i}\mathbf{24}_F\mathbf{45} \\ & + \hat{y}^{(9)}_{i}\bar{\mathbf{5}}_{F,i}\mathbf{24}_F\mathbf{70} + \hat{y}^{(10)}\mathbf{24}_F\mathbf{24}_F\mathbf{24} + \text{H.c.},\end{aligned} \quad \text{(A3)}$$

$$\hat{\mathcal{L}}_{SS} = m^2_{\mathbf{5}}\mathbf{5}\cdot\mathbf{5}^* + m^2_{\mathbf{15}}\mathbf{15}\cdot\mathbf{15}^* + m^2_{\mathbf{45}}\mathbf{45}\cdot\mathbf{45}^* + m^2_{\mathbf{50}}\mathbf{70}\cdot\mathbf{70}^* + \frac{1}{2}m^2_{\mathbf{24}}\mathbf{24}\cdot\mathbf{24}, \quad \text{(A4)}$$

$$\begin{aligned}\hat{\mathcal{L}}_{SSS} = {}& (\hat{h}^{(1)}\mathbf{5}\cdot\mathbf{5}\cdot\mathbf{15}^* + \hat{h}^{(2)}\mathbf{5}\cdot\mathbf{15}^*\cdot\mathbf{70} + \hat{h}^{(3)}\mathbf{5}\cdot\mathbf{24}\cdot\mathbf{45}^* + \hat{h}^{(4)}\mathbf{5}\cdot\mathbf{24}\cdot\mathbf{70}^* + \hat{h}^{(5)}\mathbf{15}\cdot\mathbf{45}^*\cdot\mathbf{45}^* \\ & + \hat{h}^{(6)}\mathbf{15}\cdot\mathbf{45}^*\cdot\mathbf{70}^* + \hat{h}^{(7)}\mathbf{15}\cdot\mathbf{70}^*\cdot\mathbf{70}^* + \hat{h}^{(8)}\mathbf{24}\cdot\mathbf{45}\cdot\mathbf{70}^* + \text{H.c.}) + \hat{h}^{(9)}\mathbf{5}\cdot\mathbf{5}^*\cdot\mathbf{24} \\ & + \hat{h}^{(10)}\mathbf{15}\cdot\mathbf{15}^*\cdot\mathbf{24} + \hat{h}^{(11;a)}[\mathbf{24}\cdot\mathbf{45}\cdot\mathbf{45}^*]_{a=1,2} + \hat{h}^{(12;a)}[\mathbf{70}\cdot\mathbf{70}^*\cdot\mathbf{24}]_{a=1,2} + \hat{h}^{(13)}\mathbf{24}\cdot\mathbf{24}\cdot\mathbf{24},\end{aligned} \quad \text{(A5)}$$

$$\begin{aligned}\hat{\mathcal{L}}_{SSSS} = {}& \hat{\lambda}^{(1)}\mathbf{5}\cdot\mathbf{5}\cdot\mathbf{5}^*\cdot\mathbf{70}^* + \hat{\lambda}^{(2)}\mathbf{5}\cdot\mathbf{5}\cdot\mathbf{45}^*\cdot\mathbf{70}^* + \hat{\lambda}^{(3)}\mathbf{5}\cdot\mathbf{5}^*\cdot\mathbf{45}\cdot\mathbf{70}^* + \hat{\lambda}^{(4;a)}[\mathbf{5}\cdot\mathbf{45}\cdot\mathbf{45}^*\cdot\mathbf{70}^*]_{a=1,2} \\ & + \hat{\lambda}^{(5;a)}[\mathbf{5}^*\cdot\mathbf{45}\cdot\mathbf{45}\cdot\mathbf{70}^*]_{a=1,\ldots,4} + \hat{\lambda}^{(6;a)}[\mathbf{45}\cdot\mathbf{45}\cdot\mathbf{45}^*\cdot\mathbf{70}^*]_{a=1,\ldots,5} + (\text{other terms}),\end{aligned} \quad \text{(A6)}$$

where the Yukawa couplings $\hat{y}^{(2)}_{ij}$ and $\hat{y}^{(5)}_{ij}$ are symmetric under an exchange of the (i, j) indices. The notation $[\ldots]_{a=1,2,\ldots}$ is used above to indicate the existence of multiple gauge-invariant contractions of a given product of fields. Quartic scalar couplings are numerous; therefore we do not write them all down here. The ones shown are important because, in their absence, it is possible to have a viable dark model candidate (which is the $\boldsymbol{K}$ scalar field defined in the following; see the main text). We also note in passing that, as usual in $SU(5)$, the scalar **5** and **45** are necessary to generate the Yukawa couplings $\hat{y}^{(1)}_{ij}, \ldots, \hat{y}^{(4)}_{ij}$ which in turn will allow the SM fermions to have realistic couplings to the Higgs field [which is a combination of the $SU(2)$ doublets found inside the **5** and **45**].

The $SU(5)$ gauge symmetry breaks down into $SU(3) \times SU(2) \times U(1)$ once the scalar **24** acquires a VEV in the singlet component (under the SM group). Using the same notation as in the main text, the fields which remain light—besides the SM fermions—are

$$\begin{aligned} &H \equiv \left(\mathbf{1}, \mathbf{2}, \frac{1}{2}\right) \in \mathbf{5} \quad \text{and} \quad \mathbf{45}, \\ &\boldsymbol{O} \equiv (\mathbf{8}, \mathbf{1}, 0) \in \mathbf{24}_F, \end{aligned} \tag{A7}$$

$$\begin{aligned} &\boldsymbol{T} \equiv \left(\mathbf{3}, \mathbf{2}, \frac{1}{6}\right) \in \mathbf{15}, \\ &\boldsymbol{K} \equiv \left(\mathbf{1}, \mathbf{4}, \frac{1}{2}\right) \in \mathbf{70}. \end{aligned} \tag{A8}$$

The most general form of the interaction Lagrangian (including mass terms) which one can form with these fields is as follows:

$$\mathcal{L}_{\rm int} = \mathcal{L}_{FF} + \mathcal{L}_{FFS} + \mathcal{L}_{SS} + \mathcal{L}_{SSS} + \mathcal{L}_{SSSS}, \tag{A9}$$

$$\mathcal{L}_{FF} = m_O \boldsymbol{OO}, \tag{A10}$$

$$\begin{aligned} \mathcal{L}_{FFS} = {} & y_{ij}^{(1)} Q_i u_j^c H + y_{ij}^{(2)} Q_i d_j^c H^* + y_{ij}^{(3)} L_i e_j^c H^* \\ & + y_{ij}^{(4)} L_i d_j^c \boldsymbol{T} + y_i^{(5)} Q_i \boldsymbol{O} \boldsymbol{T}^* + \text{H.c.}, \end{aligned} \tag{A11}$$

$$\mathcal{L}_{SS} = m_H^2 H H^* + m_T^2 \boldsymbol{T}\boldsymbol{T}^* + m_K^2 \boldsymbol{K}\boldsymbol{K}^*, \tag{A12}$$

$$\mathcal{L}_{SSS} = 0, \tag{A13}$$

$$\begin{aligned} \mathcal{L}_{SSSS} = {} & (\lambda^{(1)} H H H^* \boldsymbol{K}^* + \lambda^{(2)} H H \boldsymbol{K}^* \boldsymbol{K}^* + \lambda^{(3)} H \boldsymbol{T}\boldsymbol{T}^* \boldsymbol{K}^* + \lambda^{(4)} H \boldsymbol{K}\boldsymbol{K}^* \boldsymbol{K}^* + \text{H.c.}) \\ & + \lambda^{(5)} H H H^* H^* + \lambda^{(6;a)} [H H^* \boldsymbol{T}\boldsymbol{T}^*]_{a=1,2} + \lambda^{(7;a)} [H H^* \boldsymbol{K}\boldsymbol{K}^*]_{a=1,2} \\ & + \lambda^{(8;a)} [\boldsymbol{T}\boldsymbol{T}\boldsymbol{T}^* \boldsymbol{T}^*]_{a=1,2} + \lambda^{(9;a)} [\boldsymbol{T}\boldsymbol{T}^* \boldsymbol{K}\boldsymbol{K}^*]_{a=1,2} + \lambda^{(10;a)} [\boldsymbol{K}\boldsymbol{K}\boldsymbol{K}^* \boldsymbol{K}^*]_{a=1,2}. \end{aligned} \tag{A14}$$

2. Model T-II

This model contains, as usual, three copies of the left-handed fermion representations $\bar{\mathbf{5}}_F$ and $\mathbf{10}_F$ of $SU(5)$. In addition, there are complex scalars **5**, **45**, **50**, two copies of the complex scalar **15**, and one copy of the real scalars **24** and **75**. With this field content, we can write the following terms:

$$\hat{\mathcal{L}}_{\rm int} = \hat{\mathcal{L}}_{FFS} + \hat{\mathcal{L}}_{SS} + \hat{\mathcal{L}}_{SSS} + \hat{\mathcal{L}}_{SSSS}, \tag{A15}$$

$$\begin{aligned} \hat{\mathcal{L}}_{FFS} = {} & \hat{y}_{ij}^{(1)} \bar{\mathbf{5}}_{F,i} \mathbf{10}_{F,j} \mathbf{5}^* + \hat{y}_{ij}^{(2)} \mathbf{10}_{F,i} \mathbf{10}_{F,j} \mathbf{5} + \hat{y}_{ij}^{(3)} \bar{\mathbf{5}}_{F,i} \mathbf{10}_{F,j} \mathbf{45}^* + \hat{y}_{ij}^{(4)} \mathbf{10}_{F,i} \mathbf{10}_{F,j} \mathbf{45} \\ & + \hat{y}_{ijk}^{(5)} \bar{\mathbf{5}}_{F,i} \bar{\mathbf{5}}_{F,j} \mathbf{15}_k + \hat{y}_{ij}^{(6)} \mathbf{10}_{F,i} \mathbf{10}_{F,j} \mathbf{50} + \text{H.c.}, \end{aligned} \tag{A16}$$

$$\hat{\mathcal{L}}_{SS} = m_{\mathbf{5}}^2 \mathbf{5} \cdot \mathbf{5}^* + (m_{\mathbf{15}}^2)_{ij} \mathbf{15}_i \cdot \mathbf{15}_j^* + m_{\mathbf{45}}^2 \mathbf{45} \cdot \mathbf{45}^* + m_{\mathbf{50}}^2 \mathbf{50} \cdot \mathbf{50}^* + \frac{1}{2} m_{\mathbf{24}}^2 \mathbf{24} \cdot \mathbf{24} + \frac{1}{2} m_{\mathbf{75}}^2 \mathbf{75} \cdot \mathbf{75}, \tag{A17}$$

$$\begin{aligned} \hat{\mathcal{L}}_{SSS} = {} & (\hat{h}_i^{(1)} \mathbf{5} \cdot \mathbf{5} \cdot \mathbf{15}_i^* + \hat{h}_{ij}^{(2)} \mathbf{15}_i \cdot \mathbf{15}_j \cdot \mathbf{50} + \hat{h}_i^{(3)} \mathbf{15}_i \cdot \mathbf{50}^* \cdot \mathbf{50}^* + \hat{h}^{(4)} \mathbf{5} \cdot \mathbf{24} \cdot \mathbf{45}^* + \hat{h}_i^{(5)} \mathbf{15}_i \cdot \mathbf{45}^* \cdot \mathbf{45}^* \\ & + \hat{h}^{(6;a)} [\mathbf{24} \cdot \mathbf{45} \cdot \mathbf{45}^*]_{a=1,2} + \hat{h}^{(7)} \mathbf{24} \cdot \mathbf{45} \cdot \mathbf{50}^* + \hat{h}^{(8)} \mathbf{5} \cdot \mathbf{45}^* \cdot \mathbf{75} + \hat{h}^{(9)} \mathbf{5} \cdot \mathbf{50}^* \cdot \mathbf{75} \\ & + \hat{h}^{(10)} \mathbf{45} \cdot \mathbf{50}^* \cdot \mathbf{75} + \text{H.c.}) + \hat{h}^{(11)} \mathbf{5} \cdot \mathbf{5}^* \cdot \mathbf{24} + \hat{h}_{ij}^{(12)} \mathbf{15}_i \cdot \mathbf{15}_j^* \cdot \mathbf{24} + \hat{h}^{(13)} \mathbf{24} \cdot \mathbf{24} \cdot \mathbf{24} \\ & + \hat{h}^{(14)} \mathbf{50} \cdot \mathbf{50}^* \cdot \mathbf{24} + \hat{h}^{(15;a)} [\mathbf{45} \cdot \mathbf{45}^* \cdot \mathbf{75}]_{a=1,2} + \hat{h}^{(16)} \mathbf{50} \cdot \mathbf{50}^* \cdot \mathbf{75} + \hat{h}^{(17)} \mathbf{24} \cdot \mathbf{24} \cdot \mathbf{75} \\ & + \hat{h}^{(18)} \mathbf{24} \cdot \mathbf{75} \cdot \mathbf{75} + \hat{h}^{(19)} \mathbf{75} \cdot \mathbf{75} \cdot \mathbf{75}, \end{aligned} \tag{A18}$$

$$\begin{aligned} \hat{\mathcal{L}}_{SSSS} = {} & \hat{\lambda}_{ij}^{(1;a)} [\mathbf{15}_i \cdot \mathbf{15}_j \cdot \mathbf{50} \cdot \mathbf{24}]_{a=1,2} + \hat{\lambda}_{ij}^{(2)} \mathbf{15}_i \cdot \mathbf{15}_j \cdot \mathbf{50} \cdot \mathbf{75} + \hat{\lambda}_i^{(3)} \mathbf{15}_i \cdot \mathbf{50}^* \cdot \mathbf{50}^* \cdot \mathbf{24} \\ & + \hat{\lambda}_i^{(4;a)} [\mathbf{15}_i \cdot \mathbf{50}^* \cdot \mathbf{50}^* \cdot \mathbf{75}]_{a=1,2} + \hat{\lambda}_i^{(5;a)} [\mathbf{15}_i \cdot \mathbf{15}_j^* \cdot \mathbf{24} \cdot \mathbf{24}]_{a=1,2,3} + (\text{other terms}). \end{aligned} \tag{A19}$$

Under an exchange of the (i,j) flavor indices $\hat{y}^{(2)}_{ij}$, $\hat{y}^{(5)}_{ij}$, $\hat{y}^{(6)}_{ij}$, $\hat{h}^{(2)}_{ij}$, $\hat{\lambda}^{(1;1)}_{ij}$ and $\hat{\lambda}^{(2)}_{ij}$ symmetric, while $\hat{y}^{(4)}_{ij}$ and $\hat{\lambda}^{(1;2)}_{ij}$ are antisymmetric. As explained in Appendix B, the quartic couplings shown above are necessary in order to suppress neutron-antineutron oscillations in model T-II.

With the fields

$$H \equiv \left(\mathbf{1},\mathbf{2},\frac{1}{2}\right) \in \mathbf{5} \quad \text{and} \quad \mathbf{45},$$
$$\boldsymbol{T} \equiv \left(\mathbf{3},\mathbf{2},\frac{1}{6}\right), \qquad \boldsymbol{Z} \equiv \left(\mathbf{6},\mathbf{1},-\frac{2}{3}\right) \in \mathbf{15}, \tag{A20}$$

$$\boldsymbol{R} \equiv (\mathbf{1},\mathbf{1},-2), \quad \boldsymbol{X} \equiv \left(\bar{\mathbf{6}},\mathbf{3},-\frac{1}{3}\right), \quad \boldsymbol{Y} \equiv \left(\mathbf{6},\mathbf{1},\frac{4}{3}\right) \in \mathbf{50}, \tag{A21}$$

which are assumed to remain light fields after of $SU(5)$ symmetry breaking (see Appendix B), one can build the following terms (note that there are two light $\boldsymbol{T}$'s but only one $\boldsymbol{Z}$):

$$\mathcal{L}_{\rm int} = \mathcal{L}_{FFS} + \mathcal{L}_{SS} + \mathcal{L}_{SSS} + \mathcal{L}_{SSSS}, \tag{A22}$$

$$\mathcal{L}_{FFS} = y^{(1)}_{ij} Q_i u^c_j H + y^{(2)}_{ij} Q_i d^c_j H^* + y^{(3)}_{ij} L_i e^c_j H^* + y^{(4)}_{ijk} L_i d^c_j \boldsymbol{T}_k + y^{(5)}_{ij} d^c_i d^c_j \boldsymbol{Z} + y^{(6)}_{ij} e^c_i e^c_j \boldsymbol{R} + y^{(7)}_{ij} Q_i Q_j \boldsymbol{X} + y^{(8)}_{ij} u^c_i u^c_j \boldsymbol{Y} + \text{H.c.}, \tag{A23}$$

$$\mathcal{L}_{SS} = m^2_H H H^* + (m^2_T)_{ij} \boldsymbol{T}_i \boldsymbol{T}^*_j + m^2_Z \boldsymbol{Z}\boldsymbol{Z}^* + m^2_R \boldsymbol{R}\boldsymbol{R}^* + m^2_X \boldsymbol{X}\boldsymbol{X}^* + m^2_Y \boldsymbol{Y}\boldsymbol{Y}^*, \tag{A24}$$

$$\mathcal{L}_{SSS} = h^{(1)}_{ij} \boldsymbol{T}_i \boldsymbol{T}_j \boldsymbol{X} + h^{(2)} \boldsymbol{Y}\boldsymbol{Z}\boldsymbol{Z} + h^{(3)} \boldsymbol{R}^* \boldsymbol{Y}^* \boldsymbol{Z} + h^{(4)} \boldsymbol{X}^* \boldsymbol{X}^* \boldsymbol{Z} + \text{H.c.}, \tag{A25}$$

$$\begin{aligned}\mathcal{L}_{SSSS} = {} & (\lambda^{(1)} H H \boldsymbol{X}\boldsymbol{Z} + \lambda^{(2)} H H \boldsymbol{X}^* \boldsymbol{Y}^* + \lambda^{(3;a)}_{ijk} [H \boldsymbol{T}^*_i \boldsymbol{T}^*_j \boldsymbol{T}^*_k]_{a=1,2} + \lambda^{(4)}_{ij} \boldsymbol{T}_i \boldsymbol{T}_j \boldsymbol{X}^* \boldsymbol{Z} \\ & + \lambda^{(5)} \boldsymbol{R}^* \boldsymbol{Z}\boldsymbol{Z}\boldsymbol{Z} + \lambda^{(6)} \boldsymbol{R}\boldsymbol{Y}\boldsymbol{Y}\boldsymbol{Z} + \lambda^{(7;a)} [\boldsymbol{X}\boldsymbol{X}\boldsymbol{Y}\boldsymbol{Z}]_{a=1,2} + \lambda^{(8)} \boldsymbol{R}\boldsymbol{X}^* \boldsymbol{X}^* \boldsymbol{Y} + \text{H.c.}) \\ & + \lambda^{(9)} H H H^* H^* + \lambda^{(10)}_{ij} H H^* \boldsymbol{T}_i \boldsymbol{T}^*_j + \lambda^{(11)} H H^* \boldsymbol{Z}\boldsymbol{Z}^* + \lambda^{(12)} H H^* \boldsymbol{R}\boldsymbol{R}^* \\ & + \lambda^{(13;a)} [H H^* \boldsymbol{X}\boldsymbol{X}^*]_{a=1,2} + \lambda^{(14)} H H^* \boldsymbol{Y}\boldsymbol{Y}^* + \lambda^{(15;a)}_{ijkl} [\boldsymbol{T}_i \boldsymbol{T}_j \boldsymbol{T}^*_k \boldsymbol{T}^*_l]_{a=1,\ldots,4} \\ & + \lambda^{(16;a)}_{ij} [\boldsymbol{T}_i \boldsymbol{T}^*_j \boldsymbol{Z}\boldsymbol{Z}^*]_{a=1,2} + \lambda^{(17)}_{ij} \boldsymbol{R}\boldsymbol{R}^* \boldsymbol{T}_i \boldsymbol{T}^*_j + \lambda^{(18;a)}_{ij} [\boldsymbol{T}_i \boldsymbol{T}^*_j \boldsymbol{X}\boldsymbol{X}^*]_{a=1,\ldots,4} \\ & + \lambda^{(19;a)}_{ij} [\boldsymbol{T}_i \boldsymbol{T}^*_j \boldsymbol{Y}\boldsymbol{Y}^*]_{a=1,2} + \lambda^{(20;a)} [\boldsymbol{Z}\boldsymbol{Z}\boldsymbol{Z}^* \boldsymbol{Z}^*]_{a=1,2} + \lambda^{(21)} \boldsymbol{R}\boldsymbol{R}^* \boldsymbol{Z}\boldsymbol{Z}^* \\ & + \lambda^{(22;a)} [\boldsymbol{X}\boldsymbol{X}^* \boldsymbol{Z}\boldsymbol{Z}^*]_{a=1,2,3} + \lambda^{(23;a)} [\boldsymbol{Y}\boldsymbol{Y}^* \boldsymbol{Z}\boldsymbol{Z}^*]_{a=1,2,3} + \lambda^{(24)} \boldsymbol{R}\boldsymbol{R}\boldsymbol{R}^* \boldsymbol{R}^* \\ & + \lambda^{(25)} \boldsymbol{R}\boldsymbol{R}^* \boldsymbol{X}\boldsymbol{X}^* + \lambda^{(26)} \boldsymbol{R}\boldsymbol{R}^* \boldsymbol{Y}\boldsymbol{Y}^* + \lambda^{(27;a)} [\boldsymbol{X}\boldsymbol{X}\boldsymbol{X}^* \boldsymbol{X}^*]_{a=1,\ldots,5} \\ & + \lambda^{(28;a)} [\boldsymbol{X}\boldsymbol{X}^* \boldsymbol{Y}\boldsymbol{Y}^*]_{a=1,2,3} + \lambda^{(29;a)} [\boldsymbol{Y}\boldsymbol{Y}\boldsymbol{Y}^* \boldsymbol{Y}^*]_{a=1,2}. \end{aligned} \tag{A26}$$

There are the following symmetries in the parameters:

(i) $\hat{y}^{(5)}_{ij}$, $\hat{y}^{(6)}_{ij}$, $\hat{y}^{(7)}_{ij}$, $\hat{y}^{(8)}_{ij}$, $\hat{h}^{(1)}_{ij}$ and $\hat{\lambda}^{(4)}_{ij}$ are symmetric under an exchange $i \leftrightarrow j$.

(ii) $\hat{\lambda}^{(3;1)}_{ijk}$ and $\hat{\lambda}^{(3;2)}_{ijk}$ have a mixed symmetry under permutations of the three indices. What this means is that for an S_3 permutation σ, $\hat{\lambda}^{(3;1)}_{\sigma(ijk)}$ is equal to a linear combination of $\hat{\lambda}^{(3;1)}_{ijk}$ and $\hat{\lambda}^{(3;2)}_{ijk}$. The same is true for $\hat{\lambda}^{(3;2)}_{\sigma(ijk)}$.

(iii) Two of the $\hat{\lambda}^{(15;a)}_{ijkl}$ parameters are symmetric both for an exchange of the (i,j) indices as well as (k,l); the remaining two $\hat{\lambda}^{(15;a)}_{ijkl}$ are antisymmetric if we exchange the (i,j) or (k,l) indices.

APPENDIX B: FINE-TUNINGS

Some parameters which multiply gauge-invariant products of $G_{\rm SM}$ representations have relations among themselves in an $SU(5)$-symmetric theory. For example, in minimal $SU(5)$ it is well known that $y_\ell = y^T_d$ simply because $\bar{\mathbf{5}}_{F,i} \mathbf{10}_{F,j} \mathbf{5}^*$ decomposes as $(d^c_i Q_j + L_i e^c_j) H^*$ plus interactions involving the scalar color triplet, which is heavy. There is no need to consider here the overall normalization factor in the contraction of the $SU(5)$ representations but, on the other hand, the precise way of contracting the $G_{\rm SM}$ representations is important; therefore let us briefly state how $SU(2)$ and $SU(3)$ indices are contracted.

Take first $SU(2)$. In the case of two doublets, we assume $\mathbf{2}\cdot\mathbf{2}'\equiv\epsilon_{ab}\mathbf{2}_a\mathbf{2}'_b$, where ϵ is the Levi-Civita tensor (primes are used to distinguish fields transforming in the same way). If there is a triplet, one can picture its three components $\mathbf{3}_a$ (their electric charges depend on the hypercharge) as forming a matrix

$$[\mathbf{3}]_{bc}\equiv\begin{pmatrix}\mathbf{3}_3 & -\frac{1}{\sqrt{2}}\mathbf{3}_2\\ -\frac{1}{\sqrt{2}}\mathbf{3}_2 & \mathbf{3}_1\end{pmatrix}_{bc}, \tag{B1}$$

in which case $\mathbf{2}\cdot\mathbf{2}'\cdot\mathbf{3}\equiv\mathbf{2}_a\mathbf{2}'_b[\mathbf{3}]_{ab}$ and $\mathbf{2}^*\cdot\mathbf{2}'^*\cdot\mathbf{3}\equiv\epsilon_{ac}\epsilon_{bd}(\mathbf{2}^*)_c(\mathbf{2}'^*)_d[\mathbf{3}]_{ab}$.

For color indices, $\mathbf{3}\cdot\mathbf{3}'\cdot\mathbf{3}''\equiv\epsilon_{abc}\mathbf{3}_a\mathbf{3}'_b\mathbf{3}''_c$. Expressions with sextets are more easily expressed if we write the six components $\mathbf{6}_a$ as a symmetric matrix:

$$[\mathbf{6}]_{bc}\equiv\begin{pmatrix}\mathbf{6}_1 & \frac{1}{\sqrt{2}}\mathbf{6}_2 & \frac{1}{\sqrt{2}}\mathbf{6}_3\\ \frac{1}{\sqrt{2}}\mathbf{6}_2 & \mathbf{6}_4 & \frac{1}{\sqrt{2}}\mathbf{6}_5\\ \frac{1}{\sqrt{2}}\mathbf{6}_3 & \frac{1}{\sqrt{2}}\mathbf{6}_5 & \mathbf{6}_6\end{pmatrix}_{bc}. \tag{B2}$$

With this notation, $\mathbf{3}^*\cdot\mathbf{3}'^*\cdot\mathbf{6}\equiv(\mathbf{3}^*)_a(\mathbf{3}'^*)_b[\mathbf{6}]_{ab}$ and $\mathbf{6}\cdot\mathbf{6}'\cdot\mathbf{6}''\equiv\epsilon_{abc}\epsilon_{def}[\mathbf{6}]_{ad}[\mathbf{6}']_{be}[\mathbf{6}'']_{cf}$. Finally, for both $SU(2)$ and $SU(3)$ indices, $\boldsymbol{R}\cdot\boldsymbol{R}^*\equiv\boldsymbol{R}_a\cdot(\boldsymbol{R}^*)_a$ for any representation $\boldsymbol{R}$.

Having said this, we can expand some important $SU(5)$ interactions and express them in terms of the $G_{\rm SM}$ fields[8]:

$$\bar{\mathbf{5}}_{F,i}\mathbf{10}_{F,j}\mathbf{5}^*\propto(d^c_iQ_j+L_ie^c_j)H'^*+(\text{heavy}), \tag{B3}$$

$$\bar{\mathbf{5}}_{F,i}\mathbf{10}_{F,j}\mathbf{45}^*\propto(d^c_iQ_j-3L_ie^c_j)H''^*+(\text{heavy}), \tag{B4}$$

$$\mathbf{10}_{F,i}\mathbf{10}_{F,j}\mathbf{5}\propto(u^c_iQ_j+Q_iu^c_j)H'+(\text{heavy}), \tag{B5}$$

$$\mathbf{10}_{F,i}\mathbf{10}_{F,j}\mathbf{45}\propto(u^c_iQ_j-Q_iu^c_j)H''+(\text{heavy}), \tag{B6}$$

$$\bar{\mathbf{5}}_{F,i}\bar{\mathbf{5}}_{F,j}\mathbf{15}\propto(d^c_iL_j+L_id^c_j)\boldsymbol{T}-\sqrt{2}d^c_id^c_j\boldsymbol{Z}+(\text{heavy}), \tag{B7}$$

$$\mathbf{10}_{F,i}\mathbf{10}_{F,j}\mathbf{50}\propto u^c_iu^c_j\boldsymbol{Y}+Q_iQ_j\boldsymbol{X}-e^c_ie^c_j\boldsymbol{R}+(\text{heavy}), \tag{B8}$$

$$\mathbf{15}_i\mathbf{15}_j\mathbf{50}\propto\boldsymbol{T}_i\boldsymbol{T}_j\boldsymbol{X}-\boldsymbol{Z}_i\boldsymbol{Z}_j\boldsymbol{Y}+(\text{heavy}), \tag{B9}$$

$$[\mathbf{15}_i\mathbf{15}_j\mathbf{50}\langle\mathbf{24}\rangle]_1\propto\boldsymbol{T}_i\boldsymbol{T}_j\boldsymbol{X}+4\boldsymbol{Z}_i\boldsymbol{Z}_j\boldsymbol{Y}+(\text{heavy}), \tag{B10}$$

$$\mathbf{15}_i\mathbf{15}_j\mathbf{50}\langle\mathbf{75}\rangle\propto\boldsymbol{T}_i\boldsymbol{T}_j\boldsymbol{X}+\boldsymbol{Z}_i\boldsymbol{Z}_j\boldsymbol{Y}+(\text{heavy}), \tag{B11}$$

$$\mathbf{15}_i\mathbf{50}^*\mathbf{50}^*\propto\boldsymbol{Z}_i(\boldsymbol{R}^*\boldsymbol{Y}^*+\boldsymbol{Y}^*\boldsymbol{R}^*)-\boldsymbol{Z}_i\boldsymbol{X}^*\boldsymbol{X}^*+(\text{heavy}), \tag{B12}$$

$$\mathbf{15}_i\mathbf{50}^*\mathbf{50}^*\langle\mathbf{24}\rangle\propto\boldsymbol{Z}_i(\boldsymbol{R}^*\boldsymbol{Y}^*+\boldsymbol{Y}^*\boldsymbol{R}^*)-\boldsymbol{Z}_i\boldsymbol{X}^*\boldsymbol{X}^*+(\text{heavy}), \tag{B13}$$

$$\mathbf{15}_i\mathbf{50}^*\mathbf{50}^*\langle\mathbf{75}\rangle\propto2\boldsymbol{Z}_i(\boldsymbol{R}^*\boldsymbol{Y}^*+\boldsymbol{Y}^*\boldsymbol{R}^*)+\boldsymbol{Z}_i\boldsymbol{X}^*\boldsymbol{X}^*+(\text{heavy}). \tag{B14}$$

(The physical Higgs boson H is assumed to be a combination of the doublets H' and H'' contained in the **5** and **45**, respectively.) Interactions involving heavy $G_{\rm SM}$ representations are not shown.

Equations (B3)–(B6) are important for obtaining realistic SM fermions masses; the Yukawa interaction in (B7) participates in both our models, while (B8) is only present in model T-II. This latter model contains scalar trilinear interactions $\mathbf{15}\cdot\mathbf{15}\cdot\mathbf{50}$ and $\mathbf{15}\cdot\mathbf{50}^*\cdot\mathbf{50}^*$ as well, which lead to both $0\nu\beta\beta$ and neutron-antineutron oscillations. To suppress the latter process one can tune the trilinear coupling of $\mathbf{15}\cdot\mathbf{15}\cdot\mathbf{50}$ with the quartic coupling of $\mathbf{15}\cdot\mathbf{15}\cdot\mathbf{50}\cdot\langle\mathbf{24}\rangle$ given that these two field contractions have different relative group-theoretical coefficients for the $\boldsymbol{TTX}$ and $\boldsymbol{ZZY}$ interactions. This is shown in Eqs. (B9) and (B10). On the other hand, $\mathbf{15}\cdot\mathbf{50}^*\cdot\mathbf{50}^*$ and $\mathbf{15}\cdot\mathbf{50}^*\cdot\mathbf{50}^*\cdot\langle\mathbf{24}\rangle$ do share the same factors, so one must use instead the VEV of the **75** to suppress neutron-antineutron oscillations [see Eqs. (B12)–(B14)].

In both models presented in this paper, one must also make sure that it is possible, by a suitable tuning of parameters, to make the various $G_{\rm SM}$ representations light (i.e., significantly smaller than the GUT scale). We shall illustrate this here only for $\boldsymbol{T}\in\mathbf{15}$ although we have checked that the same is possible for all particles in both models. Consider then for simplicity a single copy of the **15**, which contains $\boldsymbol{T}\equiv(\mathbf{3},\mathbf{2},\frac{1}{6})$, $\boldsymbol{Z}\equiv(\mathbf{6},\mathbf{1},-\frac{2}{3})$ and $\Delta\equiv S_{\mathbf{1},\mathbf{3},1}$. Once the **24** acquires a VEV, the trilinear coupling $\mathbf{15}\cdot\mathbf{15}^*\cdot\mathbf{24}$ will contribute differently to the masses of these three $G_{\rm SM}$ representations:

$$\mathbf{15}\cdot\mathbf{15}^*\cdot\langle\mathbf{24}\rangle\propto4\boldsymbol{T}\boldsymbol{T}^*-\boldsymbol{Z}\boldsymbol{Z}^*-6\Delta\Delta^*. \tag{B15}$$

As far as quartic couplings are concerned, ignoring the scalar **75** representation (which may also acquire a VEV), one must consider three independent quartic couplings $\hat{\lambda}^{(5;a)}[\mathbf{15}\cdot\mathbf{15}^*\cdot\mathbf{24}\cdot\mathbf{24}]_{a=1,2,3}$ [confer with Eq. (A19)]. It turns out that $[\mathbf{15}\cdot\mathbf{15}^*\cdot\langle\mathbf{24}\rangle\cdot\langle\mathbf{24}\rangle]_{a=1,2,3}\propto c_{a,1}\boldsymbol{T}\boldsymbol{T}^*+c_{a,2}\boldsymbol{Z}\boldsymbol{Z}^*+c_{a,3}\Delta\Delta^*$ with the vectors $(c_{a,1},c_{a,2},c_{a,3})^T$ for $a=1,2,3$ being linearly independent so, considering that linear combinations of the three gauge-invariant contractions $[\mathbf{15}\cdot\mathbf{15}^*\cdot\mathbf{24}\cdot\mathbf{24}]_a$ are obviously gauge invariant as well, we may go ahead and define them such that

$$[\mathbf{15}\cdot\mathbf{15}^*\cdot\langle\mathbf{24}\rangle\cdot\langle\mathbf{24}\rangle]_1\propto\boldsymbol{T}\boldsymbol{T}^*, \tag{B16}$$

[8]These Georgi-Jarlskog–like factors can be computed in a systematic way with the SubgroupEmbeddingCoefficients function SUSYNO program [66]. The user needs to interpret and perhaps adapt the output with care, since the program assumes a sign and normalization convention for the contraction of $SU(5)$, $SU(2)$ and color indices which very likely differs from the one preferred by the user.

$$[\mathbf{15}\cdot\mathbf{15}^*\cdot\langle\mathbf{24}\rangle\cdot\langle\mathbf{24}\rangle]_2 \propto \boldsymbol{Z}\boldsymbol{Z}^*, \tag{B17}$$

$$[\mathbf{15}\cdot\mathbf{15}^*\cdot\langle\mathbf{24}\rangle\cdot\langle\mathbf{24}\rangle]_3 \propto \Delta\Delta^*. \tag{B18}$$

Then, at the $SU(5)$-breaking scale,

$$m_T^2 = m_{\mathbf{15}}^2 + 4\hat{h}\langle\mathbf{24}\rangle + \hat{\lambda}^{(5;1)}, \tag{B19}$$

$$m_Z^2 = m_{\mathbf{15}}^2 - \hat{h}\langle\mathbf{24}\rangle + \hat{\lambda}^{(5;2)}, \tag{B20}$$

$$m_{S_{1,3,1}}^2 = m_{\mathbf{15}}^2 - 6\hat{h}\langle\mathbf{24}\rangle + \hat{\lambda}^{(5;3)}, \tag{B21}$$

where $m_{\mathbf{15}}^2$ is the mass term of the **15** and $\hat{h}$ is the (properly normalized) trilinear coupling of $\mathbf{15}\cdot\mathbf{15}^*\cdot\mathbf{24}$ [corresponding to what we called $\hat{h}^{(10)}$ in Eqs. (A5) and $\hat{h}_{ij}^{(12)}$ in (A18)]. As such, it is clear that with an appropriate tuning of parameters, it is possible to make $\boldsymbol{T}$ and $\boldsymbol{Z}$ light while keeping Δ heavy.

APPENDIX C: DECOMPOSITION TABLE OF $SU(5)$ REPRESENTATIONS

For reference, we provide here Table I with the decomposition of $SU(5)$ representations into those of the SM group (these data coincide with the one given in [67]).

TABLE I. $SU(3)\times SU(2)\times U(1)$ decomposition of some $SU(5)$ representations. As usual, the correctly normalized hypercharge y_N is obtained by multiplying the values of y shown here by $\sqrt{\frac{3}{5}}$.

Representation	Decomposition
5	$(\mathbf{3},\mathbf{1},-\frac{1}{3})+(\mathbf{1},\mathbf{2},\frac{1}{2})$
10	$(\bar{\mathbf{3}},\mathbf{1},-\frac{2}{3})+(\mathbf{3},\mathbf{2},\frac{1}{6})+(\mathbf{1},\mathbf{1},1)$
15	$(\mathbf{6},\mathbf{1},-\frac{2}{3})+(\mathbf{3},\mathbf{2},\frac{1}{6})+(\mathbf{1},\mathbf{3},1)$
24	$(\mathbf{3},\mathbf{2},-\frac{5}{6})+(\mathbf{8},\mathbf{1},0)+(\mathbf{1},\mathbf{3},0)+(\mathbf{1},\mathbf{1},0)+(\bar{\mathbf{3}},\mathbf{2},\frac{5}{6})$
35	$(\overline{\mathbf{10}},\mathbf{1},1)+(\bar{\mathbf{6}},\mathbf{2},\frac{1}{6})+(\bar{\mathbf{3}},\mathbf{3},-\frac{2}{3})+(\mathbf{1},\mathbf{4},-\frac{3}{2})$
40	$(\mathbf{8},\mathbf{1},1)+(\bar{\mathbf{6}},\mathbf{2},\frac{1}{6})+(\mathbf{3},\mathbf{2},\frac{1}{6})+(\bar{\mathbf{3}},\mathbf{3},-\frac{2}{3})+(\bar{\mathbf{3}},\mathbf{1},-\frac{2}{3})+(\mathbf{1},\mathbf{2},-\frac{3}{2})$
45	$(\bar{\mathbf{3}},\mathbf{1},\frac{4}{3}),(\mathbf{8},\mathbf{2},\frac{1}{2}),(\mathbf{1},\mathbf{2},\frac{1}{2}),(\bar{\mathbf{6}},\mathbf{1},-\frac{1}{3}),(\mathbf{3},\mathbf{3},-\frac{1}{3}),(\mathbf{3},\mathbf{1},-\frac{1}{3}),(\bar{\mathbf{3}},\mathbf{2},-\frac{7}{6})$
50	$(\mathbf{6},\mathbf{1},\frac{4}{3})+(\mathbf{8},\mathbf{2},\frac{1}{2})+(\bar{\mathbf{6}},\mathbf{3},-\frac{1}{3})+(\mathbf{3},\mathbf{1},-\frac{1}{3})+(\bar{\mathbf{3}},\mathbf{2},-\frac{7}{6})+(\mathbf{1},\mathbf{1},-2)$
70	$(\mathbf{6},\mathbf{2},-\frac{7}{6})+(\mathbf{15},\mathbf{1},-\frac{1}{3})+(\mathbf{3},\mathbf{3},-\frac{1}{3})+(\mathbf{3},\mathbf{1},-\frac{1}{3})+(\mathbf{8},\mathbf{2},\frac{1}{2})+(\mathbf{1},\mathbf{4},\frac{1}{2})+(\mathbf{1},\mathbf{2},\frac{1}{2})+(\bar{\mathbf{3}},\mathbf{3},\frac{4}{3})$
70′	$(\overline{\mathbf{15'}},\mathbf{1},\frac{4}{3})+(\overline{\mathbf{10}},\mathbf{2},\frac{1}{2})+(\bar{\mathbf{6}},\mathbf{3},-\frac{1}{3})+(\bar{\mathbf{3}},\mathbf{4},-\frac{7}{6})+(\mathbf{1},\mathbf{5},-2)$
75	$(\bar{\mathbf{3}},\mathbf{1},-\frac{5}{3})+(\bar{\mathbf{6}},\mathbf{2},-\frac{5}{6})+(\mathbf{3},\mathbf{2},-\frac{5}{6})+(\mathbf{8},\mathbf{3},0)+(\mathbf{8},\mathbf{1},0)+(\mathbf{1},\mathbf{1},0)+(\mathbf{6},\mathbf{2},\frac{5}{6})+(\bar{\mathbf{3}},\mathbf{2},\frac{5}{6})+(\mathbf{3},\mathbf{1},\frac{5}{3})$

[1] F. F. Deppisch, M. Hirsch, and H. Päs, J. Phys. G **39**, 124007 (2012).
[2] H. Päs, M. Hirsch, H. Klapdor-Kleingrothaus, and S. Kovalenko, Phys. Lett. B **498**, 35 (2001).
[3] J. Helo, M. Hirsch, S. Kovalenko, and H. Päs, Phys. Rev. D **88**, 011901 (2013).
[4] J. Helo, M. Hirsch, H. Päs, and S. Kovalenko, Phys. Rev. D **88**, 073011 (2013).
[5] F. Bonnet, M. Hirsch, T. Ota, and W. Winter, J. High Energy Phys. 03 (2013) 055.
[6] R. Mohapatra, *Unification and Supersymmetry. The Frontiers of Quark-Lepton Physics* (Springer, New York, 1986).
[7] P. Minkowski, Phys. Lett. **67B**, 421 (1977).
[8] M. Gell-Mann, P. Ramond, and R. Slansky, *Conf. Proc.*, C790927 (1979) 315; *Supergravity Workshop 27-28 Sep 1979, Stony Brook, New York*, edited by (North-Holland, Amsterdam, 1979).
[9] T. Yanagida, *Workshop on the Baryon Number of the Universe and Unified Theories 13-14 Feb 1979, Tsukuba, Japan*, C7902131 (1979) 95.

[10] R. N. Mohapatra and G. Senjanovic, Phys. Rev. Lett. **44**, 912 (1980).
[11] J. Schechter and J. Valle, Phys. Rev. D **22**, 2227 (1980).
[12] M. Magg and C. Wetterich, Phys. Lett. **94B**, 61 (1980).
[13] R. N. Mohapatra and G. Senjanovic, Phys. Rev. D **23**, 165 (1981).
[14] T. P. Cheng and L.-F. Li, Phys. Rev. D **22**, 2860 (1980).
[15] U. Amaldi, W. de Boer, and H. Furstenau, Phys. Lett. B **260**, 447 (1991).
[16] U. Amaldi, W. de Boer, P. H. Frampton, H. Furstenau, and J. T. Liu, Phys. Lett. B **281**, 374 (1992).
[17] B. Brahmachari, U. Sarkar, and K. Sridhar, Phys. Lett. B **297**, 105 (1992).
[18] I. Dorsner and P. Fileviez Perez, Nucl. Phys. **B723**, 53 (2005).
[19] I. Dorsner, P. Fileviez Perez, and G. Rodrigo, Phys. Rev. D **75**, 125007 (2007).
[20] M. Agostini *et al.* (GERDA Collaboration), Phys. Rev. Lett. **111**, 122503 (2013).
[21] J. Albert *et al.* (EXO-200 Collaboration), Nature (London) **510**, 229 (2014).
[22] A. Gando *et al.* (KamLAND-Zen Collaboration), Phys. Rev. Lett. **110**, 062502 (2013).
[23] K. Asakura *et al.* (KamLAND-Zen Collaboration), arXiv:1409.0077.
[24] D. Forero, M. Tortola, and J. Valle, Phys. Rev. D **90**, 093006 (2014).
[25] J. Adam *et al.* (MEG Collaboration), Phys. Rev. Lett. **110**, 201801 (2013).
[26] G. Aad *et al.* (ATLAS Collaboration), Phys. Lett. B **716**, 1 (2012).
[27] S. Chatrchyan *et al.* (CMS Collaboration), Phys. Lett. B **716**, 30 (2012).
[28] L. Randall and C. Csaki, arXiv:hep-ph/9508208.
[29] H. Georgi and C. Jarlskog, Phys. Lett. **86B**, 297 (1979).
[30] K. Babu and C. N. Leung, Nucl. Phys. **B619**, 667 (2001).
[31] M. Cirelli, N. Fornengo, and A. Strumia, Nucl. Phys. **B753**, 178 (2006).
[32] K. Abe *et al.* (Super-Kamiokande Collaboration), Phys. Rev. Lett. **113**, 121802 (2014).
[33] K. Babu and R. Mohapatra, Phys. Lett. B **715**, 328 (2012).
[34] R. Mohapatra and P. Pal, Lect. Notes Phys. **60**, 1 (1998).
[35] J. W. Valle and J. C. Romão, *Neutrinos in High Energy and Astroparticle Physics* (Wiley-VCH Verlag GmbH & Co., Weinheim, 2015).
[36] S. Weinberg, Phys. Rev. Lett. **43**, 1566 (1979).
[37] D. Aristizabal Sierra, A. Degee, L. Dorame, and M. Hirsch, J. High Energy Phys. 03 (2015) 040.
[38] P. W. Angel, Y. Cai, N. L. Rodd, M. A. Schmidt, and R. R. Volkas, J. High Energy Phys. 10 (2013) 118.
[39] J. Helo, M. Hirsch, T. Ota, and F. A. P. d. Santos, J. High Energy Phys. 05 (2015) 092.
[40] K. Muto, E. Bender, and H. Klapdor, Z. Phys. A **334**, 187 (1989).
[41] A. Faessler, V. Rodin, and F. Simkovic, J. Phys. G **39**, 124006 (2012).
[42] J. Menendez, A. Poves, E. Caurier, and F. Nowacki, J. Phys. Conf. Ser. **312**, 072005 (2011).
[43] J. Stupak III (ATLAS Collaboration), Eur. Phys. J. Web Conf. **28**, 12012 (2012).
[44] G. Aad *et al.* (ATLAS Collaboration), Eur. Phys. J. C **72**, 2151 (2012).
[45] CMS Collaboration, Report No. CMS-PAS-EXO-12-041, http://cms-results.web.cern.ch/cms-results/public-results/preliminary-results/EXO-12-041/.
[46] V. Khachatryan *et al.* (CMS Collaboration), arXiv:1503.09049.
[47] V. Khachatryan *et al.* (CMS Collaboration), Phys. Lett. B **739**, 229 (2014).
[48] CMS Collaboration, Report No. CMS-PAS-EXO-12-043, http://cms-results.web.cern.ch/cms-results/public-results/preliminary-results/EXO-12-043/.
[49] F. Staub, Comput. Phys. Commun. **184**, 1792 (2013).
[50] F. Staub, Comput. Phys. Commun. **185**, 1773 (2014).
[51] F. Staub, T. Ohl, W. Porod, and C. Speckner, Comput. Phys. Commun. **183**, 2165 (2012).
[52] W. Porod, Comput. Phys. Commun. **153**, 275 (2003).
[53] W. Porod and F. Staub, Comput. Phys. Commun. **183**, 2458 (2012).
[54] J. Alwall, R. Frederix, S. Frixione, V. Hirschi, F. Maltoni, O. Mattelaer, H.-S. Shao, T. Stelzer, P. Torrielli, and M. Zaro, J. High Energy Phys. 07 (2014) 079.
[55] V. Khachatryan *et al.* (CMS Collaboration), Eur. Phys. J. C **74**, 3149 (2014).
[56] R. Mohapatra, J. Phys. G **36**, 104006 (2009).
[57] I. Phillips *et al.*, arXiv:1410.1100.
[58] C. Arbeláez, M. Hirsch, M. Malinsky, and J. C. Romão, Phys. Rev. D **89**, 035002 (2014).
[59] K. Abe *et al.*, arXiv:1109.3262.
[60] T. Han, I. Lewis, and Z. Liu, J. High Energy Phys. 12 (2010) 085.
[61] G. Aad *et al.* (ATLAS Collaboration), Phys. Rev. D **91**, 052007 (2015).
[62] V. Khachatryan *et al.* (CMS Collaboration), Phys. Rev. D **91**, 052009 (2015).
[63] G. Aad *et al.* (ATLAS Collaboration), J. High Energy Phys. 03 (2015) 041.
[64] F. F. Deppisch, J. Harz, and M. Hirsch, Phys. Rev. Lett. **112**, 221601 (2014).
[65] F. F. Deppisch, J. Harz, M. Hirsch, W.-C. Huang, and H. Päs, arXiv:1503.04825.
[66] R. M. Fonseca, Comput. Phys. Commun. **183**, 2298 (2012).
[67] R. Slansky, Phys. Rep. **79**, 1 (1981).